

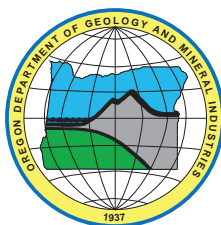
State of Oregon
Department of Geology and Mineral Industries
Vicki S. McConnell, State Geologist

Open-File Report O-08-08

**PRELIMINARY GEOLOGIC MAP OF THE MULE HILL 7.5' QUADRANGLE,
KLAMATH COUNTY, OREGON, AND SISKIYOU COUNTY, CALIFORNIA**

By

Stanley A. Mertzman¹, Richard W. Hazlett², Isaac P. Weaver³, Stephen Crabtree³,
Chris Eisinger⁴, Amy Gaffney⁴, Darren Gravely⁵, Matthew Hall³, Myra Hill⁶,
Bryan Klawiter⁷, Gordon McCreight⁸, Amber McIntosh⁴, Jennifer McIntosh⁹,
Anders Nilsson⁷, Stephanie Phippen⁷, Sarah Robinson³, Jacob Sewall¹⁰, and Jeffrey Winick³



2008

¹Franklin and Marshall College, Department of Earth and Environment, Box 3003, Lancaster, Pennsylvania 17604

²Pomona College Geology Department, 185 East 6th Street Claremont, California 91711

³Formerly at Franklin and Marshall College, Department of Earth and Environment, Box 3003, Lancaster, Pennsylvania 17604

⁴Formerly at Colorado College, Department of Geology, 14 East Cache La Poudre, Colorado Springs, Colorado 80903

⁵Formerly at Pomona College Geology Department, 185 East 6th Street, Claremont, California 91711

⁶Formerly at Williams College, Geosciences Department, Clark Hall, 947 Main Street, Williamstown, Massachusetts 01267

⁷Formerly at Carleton College, Department of Geology, Mudd Hall, Northfield, Minnesota 55057

⁸Formerly at the College of Wooster, Department of Geology, 944 College Mall, Scovel Hall Wooster, Ohio 44691

⁹Formerly at Whitman College, Department of Geology, Walla Walla, Washington 99362

¹⁰Formerly at Washington and Lee University, Department of Geology, Lexington, Virginia 24450

NOTICE

This paper is being published as received from the author(s). No warranty, expressed or implied, is made regarding the accuracy or utility of the information described and/or contained herein, nor shall the act of distribution constitute any such warranty. This disclaimer applies both to individual use of the data and aggregate use with other data. The Oregon Department of Geology and Mineral Industries shall not be held liable for improper or incorrect use of this information.

Oregon Department of Geology and Mineral Industries Open-File Report O-08-08
Published in conformance with ORS 516.030

For copies of this publication or other information about Oregon's geology and natural resources, contact:

Nature of the Northwest Information Center
800 NE Oregon Street #5
Portland, Oregon 97232
(503) 872-2750
<http://www.naturenw.org>

or these DOGAMI field offices:

Baker City Field Office
1510 Campbell St.
Baker City, OR 97814-3442
Telephone (541) 523-3133
Fax (541) 523-5992

Grants Pass Field Office
5375 Monument Drive
Grants Pass, OR 97526
Telephone (541) 476-2496
Fax (541) 474-3158

For additional information:
Administrative Offices
800 NE Oregon Street, Suite 965
Portland, OR 97232
Telephone (971) 673-1555
Fax (971) 673-1562
<http://www.oregongeology.com>
<http://egov.oregon.gov/DOGAMI/>

Introduction

The Mule Hill 7.5' quadrangle is part of the southernmost tier of quadrangles in the state of Oregon. Figure 1 provides the detailed geographic context for the Mule Hill quadrangle and the immediately surrounding area. The California-Oregon state-line crosses the southern section of the quadrangle in such a manner that Oregon constitutes approximately 90 percent of the map area while California makes up the remaining 10 percent. The Klamath River flows in a V-shaped canyon through the southeast quarter of the Mule Hill quadrangle thus providing excellent stratigraphy, particularly on the river's northern flank. The Klamath River is one of only three that transect the north-south axis of the Cascade Mountain Range. The other two through-flowing rivers are the Pit River in northern California and the well-known Columbia River that forms the boundary between the states of Oregon and Washington. A second feature that adds to the distinctiveness of the Mule Hill quadrangle is the presence of relatively older volcanic rocks that erupted during a pre-Cascade phase of Cenozoic volcanism. In the southern portion of the quadrangle, erosion by the Klamath River and its tributaries has cut down through the veneer of younger Cascade Mountain-related volcanic rocks and has exposed this basement, so to speak: older, more weathered, more altered, primarily igneous rock that is several tens of millions of years old.

Before embarking on a broad examination of the geology of the Mule Hill quadrangle, a comment on rock nomenclature is in order. When geoscientists classify igneous rock samples they often come at it from two points of view. One is based on identifying the visible minerals in a hand sample (a modal mineral classification) and the other is based on a chemical analysis of that sample (a chemical classification of igneous rocks – see Figure 2 as an example). Naturally the latter is more precise and rigorous, and the former is looser and less precise and is open to more opinions. The most common volcanic rocks (basalt, basaltic andesite, andesite, dacite, rhyolite) define a sequence in which the iron- and magnesium-bearing silicate minerals (olivine, orthopyroxene, clinopyroxene, hornblende, biotite) are most abundant on the left side of the sequence, forming upwards of 50 to 60 percent of the minerals present and decreasing to nearly zero to the right, namely, in rhyolite. The remaining 40 to 50 percent of the rock consists mostly of plagioclase feldspar, a non-iron- and magnesium-bearing silicate mineral, plus a few percent of chromium-, iron-, and titanium-dominated oxide minerals. With regard to rock chemistry, silica (SiO_2) increases from basalt to rhyolite and correlates directly with increasing viscosity and greater explosivity.

Table 1, which accompanies the geologic map of the Mule Hill quadrangle, contains the chemical and age data for all the analyzed rock samples. Figure 1 also depicts the location of all the samples for which age dates exist, both within the Mule Hill quadrangle and immediately adjacent to it. These adjacent dated-samples are depicted because they are from extensions of the volcanic rock units found within the Mule Hill map area. The goal was to show all the ages for each volcanic unit discussed below in the *Explanation of Map Units*. Figure 2 is a total alkali ($\text{Na}_2\text{O} + \text{K}_2\text{O}$) versus SiO_2 diagram that summarizes the rock names that are most germane for the volcanic materials present in this quadrangle. In addition, Figure 2 displays the chemical data of the samples from the stratigraphic units below, each of which is denoted by a unique symbol as ascribed in the accompanying legend. Lastly, Mertzman (2000) and Mertzman (unpublished data, 2007 and 2008) provide

many new ages, derived from both a whole rock K-Ar method and $^{40}\text{Ar}/^{39}\text{Ar}$ technology, that have been measured through December, 2008.

Three major phases of Cenozoic volcanism are evident in this region. The oldest phase, known as the Early Western Cascade Episode, extends from 35 to 17 Ma (late Eocene to the beginning of mid-Miocene time [Gradstein and others, 2004]), while the middle phase of volcanism is known as the Late Western Cascade Episode and covers the block of geologic time from 16.9 to 7.5 Ma (mid- to late Miocene) (Priest and others, 1983; Priest, 1990). However, evidence of this older volcanic activity is apparent only when erosion has removed the veneer of igneous rocks erupted in the third and youngest volcanic phase, the High Cascade Episode. Figure 3 is a histogram that summarizes whole rock K-Ar and $^{40}\text{Ar}/^{39}\text{Ar}$ ages determined on rock samples from the Mule Hill quadrangle in conjunction with the lead author's regional geologic mapping efforts. There is an unconformity (age gap) of nearly six million years, from 13.2 to 7.4 Ma to be exact, that characterizes the volcanic activity within the Mule Hill quadrangle. The Heppsie Formation encompasses all the volcanic material erupted during Early Western Cascade Episode, whereas the Basalt to Andesite of Hayden Creek includes all the volcanic rocks within the Late Western Cascade Episode; referring to Figure 3, there is at least a one million year gap in geologic time between these two rock units. The magnitude of this unconformity may be significantly larger perhaps by even a factor of three to four since the Heppsie Formation ages result from the whole rock K-Ar method. This age dating technique is prone to argon retention issues, particularly in those cases, such as this one, where either tuffaceous or pyroclastic volcanic materials are involved (Faure, 1986). Figure 4 builds upon the Mule Hill data displayed in Figure 3 (red color) by adding age-dated samples from the eight surrounding quadrangles (black color); the histograms end up remarkably similar in their pattern of age-date distribution. The only discrepancies fall within the 13.2 to 7.4 Ma age gap. The older two "rogue" ages are whole-rock K-Ar samples from the Secret Spring Mountain quadrangle, which is located immediately to the south of the Mule Hill quadrangle (see Figure 1). Secret Spring Mountain is a large basaltic shield volcano and the two samples in question are from areas located relatively close to the exposed shallow plutonic conduit-forming rocks exposed in the summit region of the mountain. It is relatively easy to imagine that some amount of argon gas could have been lost from these two rocks as younger magma batches were intruded into the volcano in close proximity to these samples (Faure, 1986). The youngest and third "rogue" data point is a $^{40}\text{Ar}/^{39}\text{Ar}$ age date from the Copco quadrangle, which is located to the southwest of the Mule Hill quadrangle (see Figure 1). This sample was collected in an area of dikes, lava flows, and a plug-like mass of hornblende andesite located on the north side of Copco Reservoir. The total area encompassed by these late Miocene outcrops is less than two km^2 . It is surrounded on all sides by younger volcanic rocks, thus forming a kipuka. Figure 5A provides a view of the largest outcrop north of Copco looking from the south towards Oregon and Figure 5B is a close-up of the columnar-jointed dike located on the far left (western side) of this prominent outcrop. The geochemistry of these 9 Ma old volcanic rocks strongly suggests they are best classified as part of the initial phase of the Early High Cascade Episode rather than being thought of as the absolute youngest activity associated with the waning stage of the Late Western Cascade Episode.

Erosion in the Klamath River Canyon has exposed the regional unconformity between the Late Western Cascade and the Early High Cascade Episodes of volcanism. The actual

contact is clearly and unmistakably exposed on the north side of the Klamath River Canyon, quite near the junction of the Mule Hill and Chicken Hills quadrangles (see Figure 1). Figure 6A is looking up-river to the northeast from the southernmost Mule Hill quadrangle while Figure 6B was taken from the border region of the Chicken Hills and Mule Hill quadrangles in section 9 of T41S, R6E and is oriented toward the west with a vehicle for scale. These photographs provide an overview of this picturesque area with its well-exposed geology. The nearly flat-lying lavas flowed primarily from north to south, range from 2 to nearly 10 m in thickness, and are stacked one on top of another, much like pancakes served at your local diner, with ages of the flows decreasing from the bottoms to the tops of Figures 6A and 6B. In the immediate foreground to the right of the vehicle track is the lava flow outcrop depicted in Figure 7A. This lava flow is between 2 and 3 m in thickness, is columnar jointed, is the point of origin of sample 95-26, and is located immediately above the pyroclastic flow unit (see Figure 7B) that marks the top of the Heppsie Formation in this part of Oregon. With regard to sample 95-26, I measured a whole rock K-Ar age of 7.41 ± 0.19 Ma, an age that is in quite good agreement with the age reported in Priest (1990) for the inception of the Early High Cascade Episode much further to the north in Oregon. In Figure 1 it is part of the unit Tmbkr (Basalt of the Klamath Rim) that extends in age from 7.4 to 5.5 Ma, making this unit almost entirely Upper Miocene in age (Gradstein and others, 2004). Whole rock K-Ar ages from samples 96-3, 96-5, JM97-27D, and 96-10 (the latter sample from Grizzly Butte in the southwest corner of the Chicken Hills quadrangle) pin down the youngest ages from the Tmbkr unit. A partial stratigraphic section was collected from the stack of Tmbkr flows depicted in Figures 6A and 6B, with sample 08SM-65 taken from above 95-26 and hence younger, and sample 08SM-61 taken high up on the north slope below the Grizzly Butte sample, 96-10, that is, from the top most layer in this area and sufficiently to the east to be into the Chicken Hills quadrangle. Time correlative with the youngest half of the Tmbkr lavas are the following volcanic rocks: 1) the basaltic andesite lavas of Mule Hill that were extruded between 6.2 and 5.5 Ma ago, 2) the basalts of Grizzly Mountain to the west in the Parker Mountain quadrangle that were erupted 6.5 ± 0.2 Ma, and 3) the basaltic lavas of Grenada Butte to the east in the Chicken Hills quadrangle that were extruded between 6.60 ± 0.19 Ma and 6.15 ± 0.17 Ma. Examining hand samples, thin sections, and whole rock chemical data suggests the Basalt of the Klamath Rim (Tmbkr), the Basalt of Grizzly Mountain (Tmbgm), and the Basalt of Grenada Butte (Tmbgb) are closely related to one another and likely formed through a very similar series of magmatic events. Mule Hill is the primary source vent for the more silica-rich basaltic andesite lavas that are time correlative to the basaltic activity (see Figure 8), and it is clear from the outcrop pattern that much, if not most, of the lavas flowed in a southerly direction. Younger volcanic rocks have subsequently covered whatever lavas may have flowed to the north. All of the pre-Pliocene volcanic rocks are cut by a fabric of northwest-southeast trending faults that have left a strong imprint on the present-day topography, particularly in the Chicken Hills, Spencer Creek (Mertzman, 2008a), and Surveyor Mountain (Mertzman and others, 2008b) quadrangles (see Figure 1).

In Table 1, the compendium of whole rock chemical data and K-Ar and $^{40}\text{Ar}/^{39}\text{Ar}$ ages, and in Figure 2, the $\text{Na}_2\text{O} + \text{K}_2\text{O}$ versus SiO_2 diagram, one can ascertain that data points for three of the four oldest rock units (Tmbhc: Basalt to Andesite of Hayden Creek, Tmbkr: Basalt of the Klamath Rim, and Tmbam: Basaltic Andesite of Mule Hill) plot cohesively as parallel to sub-parallel assemblages at the highest $\text{Na}_2\text{O} + \text{K}_2\text{O}$ values for a given silica

value. The fourth and actually the oldest unit, the Heppsie Formation, is markedly higher in silica than all the other Miocene-aged samples, a major point of geochemical distinction. What is abundantly clear is the existence of a general pattern in which the older rocks have higher $\text{Na}_2\text{O} + \text{K}_2\text{O}$ values and the younger rocks have lower $\text{Na}_2\text{O} + \text{K}_2\text{O}$ values (see Figure 9). To put it another way, the volcanic rocks of the Mule Hill quadrangle become less alkali-rich as a function of decreasing age. A less apparent tendency is that the volcanic rocks also become lower in silica as a function of decreasing age (see Figure 10); that is, the overall trend in regional geochemistry is from basaltic andesite to basalt and / or higher silica basalt to lower silica basalt as a function of decreasing age.

After something of a lull (see Figures 3 and 4) Pliocene volcanism commenced with the eruption of the Tpbac, the Basaltic Andesite of Camp Creek. The Pliocene Epoch (5.332 to 1.806 Ma) was a time of widespread volcanic activity. Lavas extruded during this interval range from diktytaxitic olivine basalt through basaltic andesite. Figure 9 clearly indicates that as the volcanic rocks get younger their $\text{Na}_2\text{O} + \text{K}_2\text{O}$ values continue to decline. The youngest volcanic activity recorded in the Mule Hill quadrangle is the approximately 1.79 Ma old Basalt of Long Prairie (Tpbldp), which lies virtually on the Pliocene-Pleistocene boundary at 1.806 Ma. Even younger volcanic activity occurs in the quadrangles to the north and to the east (see Figure 1).

Explanation of Map Units

Surficial Units

Qls **Landslide deposits (Pleistocene to Holocene)**—Unconsolidated volcanic breccia found in close association with the Klamath River, specifically where it has down-cut into pre-Pliocene weakly welded silicic pyroclastic rocks that have relatively thick, massive, mafic lava flows resting unconformably on top of them. Hazlett and others (1997) suggest that the unconformity is a zone of structural weakness prone to slippage of the massive, dense stack of lavas downhill under the influence of gravity given suitable friction-reducing circumstances (significant rain or melting snows to lubricate this boundary zone) coupled with a triggering mechanism like an earthquake. There exists an interesting correspondence between Klamath River flow characteristics and the presence / absence of significant landslide deposits. Until the Klamath River has cut down through the unconformity that separates the predominantly pyroclastic flow deposits that are characteristic of the top of the Heppsie Formation and the overlying, exclusively basalt lava flows of the oldest Early High Cascade stratigraphic units (i.e., the Basalt of the Klamath Rim [Tmbkr]), the rapids are exclusively class II to barely class III (See web site: Mile-by-Mile Whitewater Rafting Guide for the Upper Klamath www.klamath-river.com/uk-mile.htm). However, once the Klamath River has incised its channel down through the unconformity then rapids like the class IV+ Caldera and Hell's Corner and a raft of class IV challenges are encountered. The largest of these landslides occurred on the northwest side of Secret Spring Mountain and moved in a northwest direction. The surface upon which the landslide moved extends from the conduit of the Secret Spring volcano, which is now exposed, all the way to the Klamath River, a distance of several miles (see Figure 11A-C).

The question mark on the Mule Hill Map Plate's Time Rock Chart at the base of Qls is to clearly indicate the lack of definitive chronological information with regard to the timing of initial Qls deposition.

Volcanic Rocks

Tbv Basaltic to basaltic andesite vent deposits (Pliocene)— Poorly lithified to unconsolidated lapilli to ash-sized cinders black to brown to red with lesser amounts of similarly colored lava spatter, bombs, and scoria. These deposits mark volcanic vents areas that are often scoria or cinder cones. The question marks on the Mule Hill Map Plate's Time Rock Chart both at the base and the top of Tbv are to clearly indicate the lack of definitive chronological information with regard to the timing of initial and final Tbv extrusion.

Tpblp Basalt of Long Prairie (Middle Pliocene to Lower Pleistocene)— Similar in age to Parker Mountain, fissures opened up on the southeast side of this large composite volcano and basaltic lavas poured primarily southward eventually flowing into the Klamath River drainage. When this activity finally waned, vesicular basalt with vertically oriented platy jointing marked the vent locations. There is no mistaking Parker-Mountain-related volcanic rock with that associated with these fissure eruptions. Whereas the former are mildly porphyritic olivine two-pyroxene basaltic andesite lavas, the latter is a light to medium gray diktytaxitic (finely vesicular producing a spongy-looking texture), non-porphyritic plagioclase, olivine basalt (Philpotts, 1989). Figure 12 is a microscopic view taken with crossed polarizers of a diktytaxitic texture. Please notice the gray to white twinned plagioclase crystals projecting into the inky blackness of the vesicles. Imagine blowing up a balloon and poking one or more fingers into the thin skin of the balloon without popping it. The plagioclase crystals projected into the walls of the expanding bubbles as the magma neared the Earth's surface and the gas phase effervesced out of the liquid phase. A diktytaxitic texture reflects relatively low viscosity conditions (e.g., see pahoehoe lava flows), which are most easily established near or at the liquidus temperature of lower silica basalt (45 to 50 percent SiO₂). Lowering the temperature and / or raising the silica content dramatically increases the viscosity of the magma and a diktytaxitic vesicular texture no longer forms. The sequence of crystallization in this type of basalt is nearly always the same: spinel first, followed by olivine, plagioclase, clinopyroxene, and Fe-Ti oxide, namely titanomagnetite, last (see Figure 13). Plagioclase usually constitutes approximately 50 percent of a typical hand specimen with olivine and clinopyroxene making up 40 to 45 percent of the second half. In physical appearance the Basalt of Tom Reservoir is a dead-ringer for the Basalt of Long Prairie. However, close examination of Figure 2 clearly indicates that while these two units have quite similar silica contents, the Basalt of Tom Reservoir consistently contains a higher alkali element content. When examined in thin section the groundmass texture varies smoothly from intersertal to intergranular to subophitic to ophitic as the cooling rate of the lava slows down, which is often related to the thickness of the lava flow (see Figure 14A-C for examples of these textures). The identicalness of the silica contents of the two units leads to very similar lava flow morphologies and physical appearance of hand samples. Three whole rock K-Ar ages and one

$^{40}\text{Ar}/^{39}\text{Ar}$ age are available for this unit, 2.6 ± 0.4 Ma, 2.1 ± 0.3 Ma, 1.9 ± 0.3 Ma, and 1.79 ± 0.12 Ma. Given the limited amount of potassium present in this basalt, usually between 0.2 and 0.3 weight percent, and the relatively young age, it is quite likely the $^{40}\text{Ar}/^{39}\text{Ar}$ age is closer to the actual time of eruption and cooling than are the whole rock K-Ar ages.

Tpbapm Basaltic Andesite of Parker Mountain— (Middle Pliocene to Lower Pleistocene) Parker Mountain is a composite volcano located in the northern half of the Parker Mountain quadrangle, which is directly west of the Mule Hill quadrangle (see Figure 1). Lavas, which have emanated from the summit region, extend outward in all directions and have flowed into the westernmost sections of the Mule Hill quadrangle. These lavas are medium gray with 8 to 10 percent plagioclase present forming rectangular-shaped crystals 1 to 2 mm in diameter. A lesser amount of olivine is present (3 to 5 percent) in somewhat larger crystals (2 to 4 mm in diameter) forming scattered glomeroporphyritic clumps of the two minerals. Each Parker Mountain hand sample examined contains 5 to 10 easily visible clumps of plagioclase and olivine. Finer grained matrix-forming minerals include much additional plagioclase together with 25 to 30 percent pyroxene and 5 to 7 percent scattered granules of titanomagnetite and olivine. Much of the olivine has rims and veins of secondary iddingsite development, a clear sign of hydrothermal alteration. Iddingsite is a product of olivine's exposure to a vapor-phase that contains both O_2 and H_2O at a relatively low to moderate temperature, 300 to 500°C (Baker and Haggerty, 1967). Iddingsite is not a mineral per se: it is a mineral assemblage that can include nontronite (an Fe-rich clay mineral), Fe-rich oxides and hydroxides that are mostly amorphous, and a silica phase. In those portions of lava flows where cooling was relatively fast and in pyroclastic material, pyroxene is confined to the matrix in crystals that are <0.5 mm in diameter. The size of the matrix-forming minerals is variable due to the cooling rate of the lava constituting the flow. If the lava flow is thicker and the sample is from the central portion, then the average size of the matrix forming minerals will be larger; thinner flows result in faster cooling and small-sized matrix-forming minerals. The pyroxene in the matrix includes both ortho- and clinopyroxene. Two whole rock K-Ar ages are available for this unit, 2.48 ± 0.50 Ma and 1.8 ± 0.2 Ma. Both samples (95-34 and 97-41) are from the Parker Mountain quadrangle (see Figure 1 for the exact locations).

Tpbms Basalt of Mud Spring Mountain (Middle to Upper Pliocene)— Vents for the Basalt of Mud Spring Mountain are a series of scoria and cinder cones, stretched out primarily in a north-south direction, that give rise to at least seven distinct but clearly related lava flow units. The geochemistry of this unit in terms of nomenclature (see Figure 2) is directly on the cusp between basalt and basaltic andesite. Outcrops are characterized by widespread flow jointing and spheroidally weathered, reddish brown boulders that are often vesicular (see Figure 15A and B). Several cinder pits are located within the vent areas of the Basalt of Mud Spring Mountain and were used as a source of road-building materials for a number of logging roads. Thin sections from pyroclastic material collected from these pits provide clear evidence with regard to what happens to the mineral olivine when exposed to quite high temperatures in an oxidizing environment. Most frequently in

this unit olivine and plagioclase occur together in glomeroporphyritic clumps 1 to 3 mm in diameter. The olivine, rather than being its typical green color, is iridescent in purple to black due to pervasive high-temperature oxidation. In thin section the olivine appears like something akin to wormy wood with magnetite exsolving out of what used to be primary olivine (see Figure 16A and B). This process of exsolution is caused by exposure of olivine, which contains Fe^{+2} but no Fe^{+3} , to hot vapor that has some air mixed in with it. Air, due to its nearly 21 percent O_2 content, rapidly converts the Fe^{+2} to Fe^{+3} . However, the Fe^{+3} does not fit into the olivine mineral structure; therefore, the no-longer-stable olivine breaks down to form two minerals, magnetite (FeFe_2O_4) and the Mg-rich orthopyroxene, enstatite (Haggerty and Baker, 1967). The plagioclase crystals show little adverse effect from the high-temperature oxidation process, quite likely because this mineral contains very little iron. In lava thin sections, olivine is characteristically partially altered to iddingsite, poikilitically encloses a few euhedral spinel crystals, and quite commonly occurs in glomeroporphyritic clumps with plagioclase 2 to 3 mm across. Even though olivine is the most apparent ferromagnesian mineral, it is not the most abundant. Clinopyroxene is, occurring with plagioclase as the dominant matrix-forming minerals, together composing nearly 80 to 85 percent of a typical lava specimen. One whole rock K-Ar age (see Figure 1, sample 95-30) is available for this unit, 2.57 ± 0.24 Ma, and it is located within the Mule Hill quadrangle.

Tpbsc Basalt of Sheepy Creek (Middle to Upper Pliocene)— The vents for the Basalt of Sheepy Creek are a set of fissures aligned in a NNW-SSE direction. These vents are a series of scoria / spatter cone structures and one main cinder cone located in the extreme southwest corner of the northerly-adjacent Surveyor Mountain quadrangle (see Figure 1). The cinder cone has been excavated by the State of Oregon as a source of aggregate for road building purposes. This quarrying activity has exposed some of the internal plumbing system through which the basaltic magma moved to the Earth's surface. Figures 2 and 3 in Mertzman and others, (2008b) illustrate the geology unearthed by the quarry activity—a vertically oriented dike cutting through crudely layered pyroclastic material that ranges in size from ash at the fine grained end of the size spectrum to bombs at the coarse end. In terms of hand specimen mineralogy at the vents, 8 to 10 percent phenocrysts of plagioclase feldspar and olivine are present and form singular crystals and glomeroporphyritic clumps 1 to 4 mm in diameter. Due to pervasive high-temperature oxidation, the olivine is iridescent in purple to black. In thin section the olivine appears like something akin to wormy wood with magnetite exsolving out of what used to be primary olivine (see Figure 16A and B). Lava flows of Sheepy Creek basalt have the same phenocryst mineralogy as the vent facies rocks, but with olivine more abundant than plagioclase feldspar. The olivine has not been affected by high-temperature alteration, but rather by primarily low-temperature processes that have produced the secondary mineral assemblage known as iddingsite. Iddingsite is brown and is found filling the fractures that cut through many of the olivine phenocrysts. It is frequently encountered as a corona around the perimeter of the olivine crystals (Baker and Haggerty, 1967). With the exception of small opaque mineral grains enclosed within early-formed olivine crystals, titanomagnetite is largely confined to the groundmass. Pyroxene is also mostly found in the groundmass crystallizing after both plagioclase and olivine. One $^{40}\text{Ar}/^{39}\text{Ar}$ age is

available for the Basalt of Sheepy Creek, and it is 2.6 ± 0.2 Ma. The sample (03SM-75) is from the eastern margin of the Little Chinquapin Mountain quadrangle (see Figure 1). One K-Ar whole rock age date is also available for the Basalt of Sheepy Creek; it is 2.4 ± 0.2 Ma and is from the Mule Hill quadrangle (see Figure 1, sample 97-22).

Tpbab Basaltic Andesite of Buck Mountain (Middle Pliocene)—The Buck Mountain composite volcano is centered in the southeast section of the adjoining Surveyor Mountain quadrangle (see Figure 1) and is segmented by NW-SE trending normal faults. Most of the lava flows within this unit are medium gray moderately porphyritic basaltic andesite, but there are several basaltic lava flows intercalated amongst them. Phenocrysts constitute 10 to 12 percent of a typical hand specimen, forming 1 to 3 mm in diameter crystals that are dominated by plagioclase with olivine constituting only 3 to 4 percent. The olivine has been marginally altered to iddingsite, which also permeates through the fractures present in the crystals. In the more mafic basaltic lavas olivine is the more abundant phenocryst-forming phase, and plagioclase takes on a more secondary role. In either instance the matrix is dominated by plagioclase with a smaller amount of pyroxene, both ortho- and clinopyroxene, together with approximately 5 to 10 percent titanomagnetite and 3 to 5 percent olivine. Much of the matrix-forming plagioclase is lath-like to acicular in crystal form. One whole rock K-Ar age is available for the Basaltic Andesite of Buck Mountain that was determined on a sample from the adjacent Surveyor Mountain quadrangle (see Figure 1, sample 95-46). The measured age is 2.76 ± 0.16 Ma. It is abundantly clear that the pervasive faulting that cuts through both Buck Mountain and Surveyor Mountain post-dates the last eruptions associated with these volcanoes. Therefore the faulting activity has to be < 1.8 Ma and Pleistocene in age.

Tpbtr Basalt of Tom Reservoir (Lower to Upper Pliocene)—The geographic feature “Tom Reservoir” is located a few miles to the southwest from the northeast corner of the Mule Hill quadrangle. Light gray aphanitic lava, often denoted by two distinct sizes of vesicles, the larger 3 to 10 mm in diameter and the smaller the size of a head of a pin, gives each hand sample a spongy appearance. This physical characteristic is defined as a diktytaxitic texture. If samples are magnified through a hand lens, plagioclase feldspar grains projecting in and through the walls of the vesicle can be seen. In hand sample these diktytaxitic basalts are fine grained, with all mineral constituents ≤ 1 mm in diameter. With regard to physical appearance, either plagioclase feldspar or olivine may form slightly larger crystals and therefore be more noticeable. Plagioclase forms nearly 50 percent of these lavas, while olivine constitutes 20 to 25 percent and clinopyroxene another 20 percent. The remaining 5 to 10 percent is made up of spinel/chromite, most often seen as inclusions in early-formed olivine crystals, and titanomagnetite, found scattered about in the matrix together with the clinopyroxene. Fieldwork has confirmed that all of the lava flows that constitute the Basalt of Tom Reservoir have been extruded from dikes vented onto the Earth’s surface. These fissure-erupted lava flows follow a gully pattern, forming ribbons of lava that do not necessarily coalesce to form sheet-like masses. Several millions of years of erosion make it devilishly difficult to trace some of these “lava streams” back to their vents. One $^{40}\text{Ar}/^{39}\text{Ar}$ age, 2.49 ± 0.06 Ma, and five whole-rock K-Ar ages (3.66 ± 0.24 , 3.26 ± 0.16 , 3.2 ± 0.2 , 2.27 ± 0.24 and 2.26 ± 0.26

Ma) are available for the Basalt of Tom Reservoir. The $^{40}\text{Ar}/^{39}\text{Ar}$ age comes from a sample located in the Spencer Creek quadrangle (see 00-91 in Figure 1); the five whole-rock K-Ar ages are from Mule Hill quadrangle samples (see CW6-9, 97-35, 97-46, 95-77, and 95-33 in Figure 1 respectively).

Tpbgb Basalt of Grouse Butte (Lower to Middle Pliocene)— The Grouse Butte scoria cone / cinder cone complex is located in the southwestern part of the Surveyor Mountain quadrangle. In hand sample the most noticeable feature is that plagioclase feldspar and olivine phenocrysts are nearly equal in abundance and size, 8 to 10 percent and 1 to 3 mm, respectively. These two minerals exist as individual mineral grains and in glomeroporphyritic clumps that can reach 5 mm in diameter. Every olivine phenocryst contains one or more quite small opaque mineral grains as inclusions within the larger olivine. This texture is referred to as poikilitic and indicates the opaque mineral crystallized first from the magma and at some later time the olivine solidified around it. The opaque grains are most likely members of the spinel solid solution series, the general formula for which is AB_2O_4 . Mineral examples include spinel (MgAl_2O_4), titanomagnetite ($\text{Fe}(\text{Fe},\text{Ti})_2\text{O}_4$), and chromite (FeCr_2O_4). Along both fractures that cut across the olivine phenocrysts at a 90° angle to the crystal's direction of elongation and around the perimeter of the grains, the olivine has been altered to the yellow-brown to dark brown secondary mineral assemblage known as iddingsite. In those portions of lava flows where cooling was relatively fast and in pyroclastic material, pyroxene is confined to the matrix in crystals that are <0.5 mm in diameter. Plagioclase, which is more abundant than the pyroxene in the matrix, forms elongated rectangular shaped crystals called laths that are flow aligned, thus forming the texture known as trachytic. Small 0.1 mm granular opaque mineral grains are peppered through the matrix forming 5 to 7 percent of the rock-forming mineral population. In the more slowly cooled portions of lava flows the augite-dominated pyroxene minerals are larger in size, typically 0.5 to 0.7 mm in diameter, and form microphenocrysts. One whole rock K-Ar age is available for this unit, 3.7 ± 0.3 Ma, and it is from sample 97-28 that is located within the Surveyor Mountain quadrangle.

Tpbah Basaltic Andesite of Hayden Mountain (Lower to Middle Pliocene)— Driving west on Oregon state highway 66 and crossing the Klamath River, the road out of the valley ascends one of the prominent northwest-southeast trending fault scarps through the use of switchbacks. The long climb ends at Hayden Summit, and just to the south is Hayden Mountain, which at first glance is a cluster of coalescing high points rather than one individual high point as at Mule Hill. Each of the quite similar-looking high points at Hayden Mountain is a scoria or cinder cone (see cinder pit 0.8 km east of Hayden Mountain) from which has emanated quite similar-looking basaltic andesite lavas. Hayden Mountain lavas have several percent of plagioclase-olivine glomeroporphyritic clumps that are 2 to 3 mm in diameter with the backdrop being 10 to 12 percent 1 mm plagioclase laths embedded in a finer matrix of plagioclase and pyroxene crystals. Even though there are no crystals of pyroxene larger than 0.4 mm, pyroxene constitutes 25 to 30 percent of the lava. Prominent faults oriented in a northwest-southeast direction cut through and displace lava flows of Hayden Mountain basaltic andesite and therefore must be younger than middle Pliocene in age. Three whole rock K-Ar ages (see samples 95-71, 97-51, and

95-28) are available for this unit with ages of 3.83 ± 0.32 , 3.7 ± 0.1 , and 3.69 ± 0.11 Ma, respectively. All three samples were collected within the Chicken Hills quadrangle (see Figure 1).

Tpbac Basaltic Andesite of Camp Creek (Lower to Middle Pliocene)— This unit can be found at the southern margin of the Surveyor Mountain map and spreads out southward and eastward into the Mule Hill, Spencer Creek, and Chicken Hills quadrangles (see Figure 1). Hand samples are characteristically light to medium gray and have 20 to 25 percent plagioclase phenocrysts that are 1 to 4 mm in diameter. Besides being notable for the pronounced porphyritic texture, these basaltic andesite lavas are somewhat unusual in that they contain nearly equal amounts of olivine and clinopyroxene phenocrysts (2 to 3 percent of each mineral) that range from 1 to rarely 3 mm in diameter. The olivine is substantially altered to iddingsite while the clinopyroxene is pristine. Glomeroporphyritic clumps up to 5 mm across are dominated by clinopyroxene with only minor amounts of plagioclase, olivine, and orthopyroxene present. These features make the Basaltic Andesite of Camp Creek relatively easy to identify. If this were not enough, at outcrops the Basaltic Andesite of Camp Creek exhibits distinctive well-developed spheroidal weathering patterns. In areas that have been heavily logged, the surface is littered with rounded to ellipsoidal boulders 0.5 to 1 m in diameter. Two whole rock K-Ar ages (S97-87 and 95-77) and one $^{40}\text{Ar}/^{39}\text{Ar}$ age (S97-73) are available. The K-Ar ages are 3.79 ± 0.10 and 3.44 ± 0.12 Ma, and the $^{40}\text{Ar}/^{39}\text{Ar}$ age is 3.85 ± 0.10 Ma. All three samples are from the Mule Hill quadrangle (see Figure 1).

Tmbam Basaltic Andesite of Mule Hill (Upper Miocene to Lower Pliocene)— The remnant of the Mule Hill volcano can be found in the northeast corner of the Mule Hill quadrangle just to the south of Oregon highway 66 (see Figure 1). Vestiges of an old fire lookout tower can be seen at the summit of Mule Hill. Since Mule Hill and its related lava flows are cut off and surrounded on all sides by younger volcanic material, it forms a kipuka, a Hawaiian term meaning an island-like area of older material surrounded by later lavas (Stearns, 1985). A hand specimen of Mule Hill lava is distinctive compared to most other lavas that crop out in this quadrangle. Scattered large solitary plagioclase phenocrysts, not in clumps with olivine, range between 3 and 5 mm in largest dimension. Dominant are the 15 to 20 percent plagioclase phenocrysts present in a typical sample with several percent smaller pyroxenes followed by a percent or so of olivine. The olivine is much more dark brown than green due to low temperature alteration to iddingsite (Baker and Haggerty, 1976). Corroborating petrographic evidence is presented in Figure 17A and B). Two whole rock K-Ar ages (see samples 95-29 and S97-62) are available for this unit, 6.24 ± 0.17 and 5.5 ± 0.2 Ma, and they are both located in the Mule Hill quadrangle.

Tmbgm Basalt of Grizzly Mountain (Upper Miocene)— Grizzly Mountain is located in the Parker Mountain quadrangle to the west of Long Prairie Creek that flows through the northwest quadrant of the Mule Hill quadrangle (see Figure 1). It is an eroded basaltic volcanic complex stretched out in a north-south orientation. Several high points denote the top of Grizzly Mountain and an abandoned road

material quarry has been dug into the south-facing side of the northern-most high point. The excavation has exposed a 7 to 8 m wide vertical dike striking essentially N-S that cuts through a series of moderately well bedded basaltic pyroclastics that are quite similar in mineralogy to that of the dike. A somewhat thicker soil cover and well-developed exfoliation features are two clues to the somewhat older age of this volcanic center's activity. In hand sample this lava is olivine basalt with 5 to 7 percent of partially to completely altered olivine phenocrysts that are 1 to 3 mm in diameter (see Figure 18). These brownish rather than greenish colored phenocrysts are present in glomeroporphyritic clumps as well as individual crystals. Plagioclase feldspar and clinopyroxene dominate the groundmass of these basaltic rocks with ~5 percent small opaque crystals all less than 0.1 mm in diameter peppered through the matrix. One whole rock K-Ar age (see sample 97-16) is available for this unit, 6.5 ± 0.2 Ma, and it is located within the Parker Mountain quadrangle (see Figure 1).

Tmbkr Basalt of the Klamath Rim (Upper Miocene)— The lava flows that constitute the Basalt of the Klamath Rim are characteristically olivine-phyric; that is, individual phenocrysts and glomeroporphyritic clumps of olivine 1 to 4 mm in diameter are visible in hand-sized specimens of these lavas. These larger sized early-formed crystals typically constitute 5 to 15 percent of a rock sample. Upon microscopic examination (See Figure 19A and B) several notable features become evident. Darker colored, small, isotropic, subhedral to euhedral spinel crystals are poikilitically enclosed within the olivine phenocryst, indicating it was actually the first mineral to solidify from the magma. Olivine crystallized after the spinel and grew around it, thus providing us with clearly interpretable evidence concerning the sequence of crystallization. A second feature to note is the dark rim around the olivine crystals that also seems to penetrate into the fractures and cracks within the olivine. This dark brown material is a post-solidification alteration product of olivine known as iddingsite (See Figure 19A and B). It is the result of both low-temperature hydration and oxidation chemical reactions (Baker and Haggerty, 1967). Plagioclase is the most abundant groundmass-forming mineral followed by pyroxene (mostly clinopyroxene) and a Fe-Ti rich opaque oxide phase known as titanomagnetite. Presently, no source vents for the Basalt of the Klamath Rim have been identified. Large volcanic vent structures have been identified at Grenada Butte and Grizzly Mountain that are similar in age to the Tmbkr lavas, but younger volcanic rocks that preclude establishing a direct connection have covered the intervening region. It should be noted, however, that the mineralogy and whole rock chemistry (see Table 1) of these three units are quite similar, and it appears plausible that they could have been related to one regional magmatic event. Six whole rock K-Ar ages (see samples 95-26, 95-74, 96-10, 96-3, JM97-27D, and 96-5) are available for this unit, 7.41 ± 0.19 , 6.15 ± 0.17 , 5.9 ± 0.2 , 5.8 ± 0.2 , 5.83 ± 0.15 , and 5.55 ± 0.18 Ma, and all but 95-74 and 96-10 (Chicken Hills quadrangle) are located in the Mule Hill quadrangle.

Tmbhc Basalt to Andesite of Hayden Creek (Middle Miocene)— The Basalt to Andesite of Hayden Creek is a geologic enigma lurking in the southern Oregonian Cascade Mountains. In the region that stretches from the California – Oregon border north to Crater Lake National Park there is no other occurrence of similarly aged volcanic rocks on the west side of the main axis of the Cascade Mountains. The unconformity that marks the upper stratigraphic boundary of the Heppsie Formation

also marks the close of the Early Western Cascade Episode of Priest (1990). In most areas this unconformity extends to the beginning of the Early High Cascade Episode between 7 and 8 Ma ago (Priest, 1990). However, from the Mule Hill quadrangle south into northern-most California this time gap is interrupted by a period of volcanism that is mostly focused between 15 and 13 Ma (Mertzman, 2000).

On the outcrop there are subtle clues available that make one suspicious that all is not what it seems to be. No pyroclastic flow material is present as is typical of the youngest portion of the Heppsie Formation. The volcanic rocks themselves seem more weathered and the outcrop pattern more subdued than is usual for extrusive rocks belonging to the Early High Cascade Episode of volcanism. So it was not a total surprise when the initial whole rock K-Ar dates were measured and ages between 15 and 13 Ma resulted. In thin section the basaltic rocks have up to 10 percent olivine phenocrysts that are partially to completely converted to iddingsite through low temperature oxidation and hydration chemical reactions (See Figure 20). The vesicles present in the tops and bottoms of lava flows are lined to occasionally partially filled with secondary minerals (primarily calcite), a characteristic that differs from the often completely filled vesicles in the rocks of the older Heppsie Formation. In the more siliceous andesite lavas, pyroxene and olivine are present as phenocrysts 0.5 to 2 mm in diameter, but these olivines have suffered through complete conversion to iddingsite while the pyroxene crystals, due to their greater stability at lower temperatures, show no vestige of alteration (see Figure 21). Five whole rock K-Ar ages (see samples CW6-9, S97-21, 96-7, 96-6, and 96-8) are available for this unit. The measured K-Ar ages are 15.0 ± 0.4 , 14.6 ± 0.9 , 14.5 ± 0.5 , 13.5 ± 0.4 , and 13.2 ± 0.3 Ma. All five samples are located in the Mule Hill quadrangle.

Tmvhf Heppsie Formation (Lower Miocene)— The Heppsie Formation constitutes the youngest portion of the Little Butte Volcanic Series. In this segment of the formation's outcrop area the older extrusive rocks are dominated by basalt, basaltic andesite, and andesite lava flows whereas in the younger, upper portion, poorly to moderately welded pyroclastic flows and air-fall tuffaceous material dominate. These latter extrusive materials range from andesite to dacite to nearly rhyolite in terms of their bulk composition (see Figure 2). On the outcrop the lavas are greenish-brown in surface coloration often with several meters or more of soil developed in situ. In the more mafic lava flows of this formation the dominant ferromagnesian minerals, olivine and pyroxene, have reacted very differently to changing physical and chemical conditions. Whereas olivine has quite often been totally converted to iddingsite as a result of relatively low temperature oxidation and hydration, pyroxene has been quite stable and shows little if any sign of alteration (See Figure 22A and B). The most abundant mineral present in these lavas is the nonferromagnesian mineral plagioclase feldspar. It is often unaltered, but in numerous locations it is cut by small cracks and veins filled by sericite mica and calcite plus a little quartz (?).

The ash flow tuff member of the Heppsie Formation is often found exposed on steep landslide scarps. There is in fact a good reason for this: due to the Heppsie Formation's inherent structural weakness, numerous landslides and slumps have

their beginnings at or near the contact between younger more massive basaltic lava flows and the Heppsie's underlying older poorly welded ash flow tuffs. In the Robinson Butte quadrangle several good examples of arcuate headwall slump structures can be easily found in the canyon of the South Fork of the Little Butte Creek. As one road-building civil engineer said to me (S.A.M.) two summers ago while working on a bridge replacement project across the South Fork, "Nothing in this valley is actually stable. Everything is moving downhill pretty fast, particularly in the spring as the winter snows melt." Also, numerous excellent examples of landslides / slump development can be found in the Klamath River canyon along the California–Oregon border beginning just below the John C. Boyle Powerhouse at what is known as the Caldera Rapid. In this region a very similar layering of geologic rock units occurs as in the South Fork of the Little Butte Creek: older siliceous poorly welded tuffaceous material is overlain by younger thick occurrences of mafic lava flows. It is likely that the same mechanism of slope failure is occurring in both areas, giving rise to landslides / slumps that set the stage for rapids to form in the streams that are flowing through the valleys. Seven ages for various Heppsie Formation samples, both whole rock K-Ar and $^{40}\text{Ar}/^{39}\text{Ar}$ ages, are available. One sample (03SM-11) with a $^{40}\text{Ar}/^{39}\text{Ar}$ age date is from the Little Chinquapin Mountain quadrangle. Its age is 22.77 ± 0.13 Ma. A second sample (03SM-21) with a $^{40}\text{Ar}/^{39}\text{Ar}$ age is from just across the boundary into the Hyatt Reservoir quadrangle. This sample was taken from a small abandoned hillside quarry. Its age was 21.73 ± 0.14 Ma. Five whole rock ages including 21.0 ± 0.5 Ma (Anders-1), 21.6 ± 0.5 Ma (97-37), 21.17 ± 0.54 Ma (A73), 17.6 ± 0.7 Ma (97-55), and 17.1 ± 0.8 Ma (97-54Z) are available and their locations can be found in Figure 1. Since the K-Ar whole rock ages are more susceptible to alteration and weathering processes (please note all Heppsie Formation K-Ar ages are \leq $^{40}\text{Ar}/^{39}\text{Ar}$ ages) the $^{40}\text{Ar}/^{39}\text{Ar}$ data are likely to be more accurate (Faure, 1986).

Acknowledgments I thank Isaac Weaver for his on-going help and cheerful support in bringing this geologic map to closure. His computer skills, particularly with regard to MapInfo and Adobe Illustrator, have been particularly valuable. I also thank Karen Mertzman for all her efforts in the X-ray lab, carefully preparing and analyzing countless samples on my behalf. I thank the Keck Foundation for its generous support of the Keck Geology Consortium over the years. I thank Franklin and Marshall College for its generous support of fieldwork over the past decade that has led to the completion of this geologic map. Support from the NSF and Franklin and Marshall College to facilitate the operation of the XRF laboratory in the Earth and Environment Department is greatly appreciated.

References

- Baker, I. and Haggerty, S. E., 1967, The alteration of olivine in basaltic and associated lavas, Part II: Intermediate and low-temperature alteration, *Contr. Mineral. and Petrol.* v. 16, 258-273.
- Faure, G., 1986, *Principles of Isotope Geology*, 2nd Edition: New York, John Wiley & Sons, Inc., 589 p.

Gradstein, F., Ogg, J., and Smith, A. ed. 2004. *A Geologic Time Scale 2004*. Cambridge, Cambridge University Press, 589p.

Haggerty, S. E. and Baker, I., 1967, The alteration of olivine in basaltic and associated lavas, Part 1: high-temperature alteration, *Contr. Mineral. and Petrol.*, v. 16, 233-257.

Hazlett, R., Bilstrom, E., Cross, B., Kormeier, G., and Mertzman, S, 1997, Widespread Late Pleistocene Landsliding Event in the Area of Secret Spring Volcano, Southern Oregon Abstracts with Program 1997 Geological Society of America Meeting, Salt Lake City, Utah.

Le Maitre, R. W. ed. 2002. *Igneous Rocks: A Classification and Glossary of Terms*. 2d ed. Cambridge: Cambridge University Press, 252p.

Mertzman, S. A., 2000, K-Ar results from the southern Oregon-northern California Cascade Range, *Oregon Geology*, v. 62, 99-122.

Mertzman, Stanley A., 2008a, Preliminary Geologic Map of the Spencer Creek 7.5' Quadrangle, Klamath County, Oregon: Oregon Department of Geology & Mineral Industries Open File Report O-08-1.

Mertzman, Stanley A., Schiffer, Ben, and Reuer, Matthew, 2008b, Preliminary Geologic Map of the Surveyor Mountain 7.5' Quadrangle, Klamath County, Oregon: Oregon Department of Geology & Mineral Industries Open File Report O-08-3.

Mile-by-Mile Whitewater Rafting Guide for the Upper Klamath (Excerpted from California Whitewater by Jim Cassady and Fryar Calhoun). Last accessed on February 12, 2009: <<http://www.klamath-river.com/uk-mile.htm>>.

Philpotts, A. R., 1989, *Petrography of Igneous and Metamorphic Rocks*: Illinois, Waveland Press, Inc, 178p.

Priest, G. R., 1990, Volcanic and tectonic evolution of the Cascade volcanic arc, central Oregon, *J. Geophys. Res.*, v. 95, 19583-19599.

Priest, G. R., Woller, N. M., Black, G. L., and Evans, S. H., 1983, Overview of the geology of the central Oregon Cascade Range, *Geology and Geothermal Resources of the Central Oregon Cascade Range*, edited by G. R. Priest and B. F. Vogt, *Spec. Pap. Oregon Department of Geology and Mineral Industries*, 15, 3-28.

Stearns, H. T., 1985, *Geology of the State of Hawaii*, 2nd Edition: California, Pacific Books, Publishers, 335p.

U.S. Geological Survey, 2006 (June 9), Upper Klamath Basin ground-water study: Background. Retrieved December 2, 2007, from <http://or.water.usgs.gov/projs_dir/or180/background.html>.

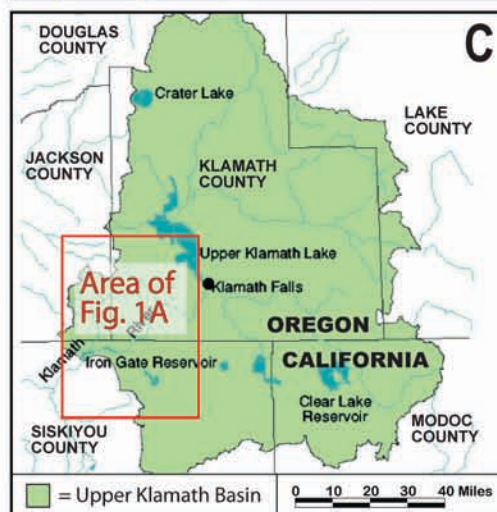
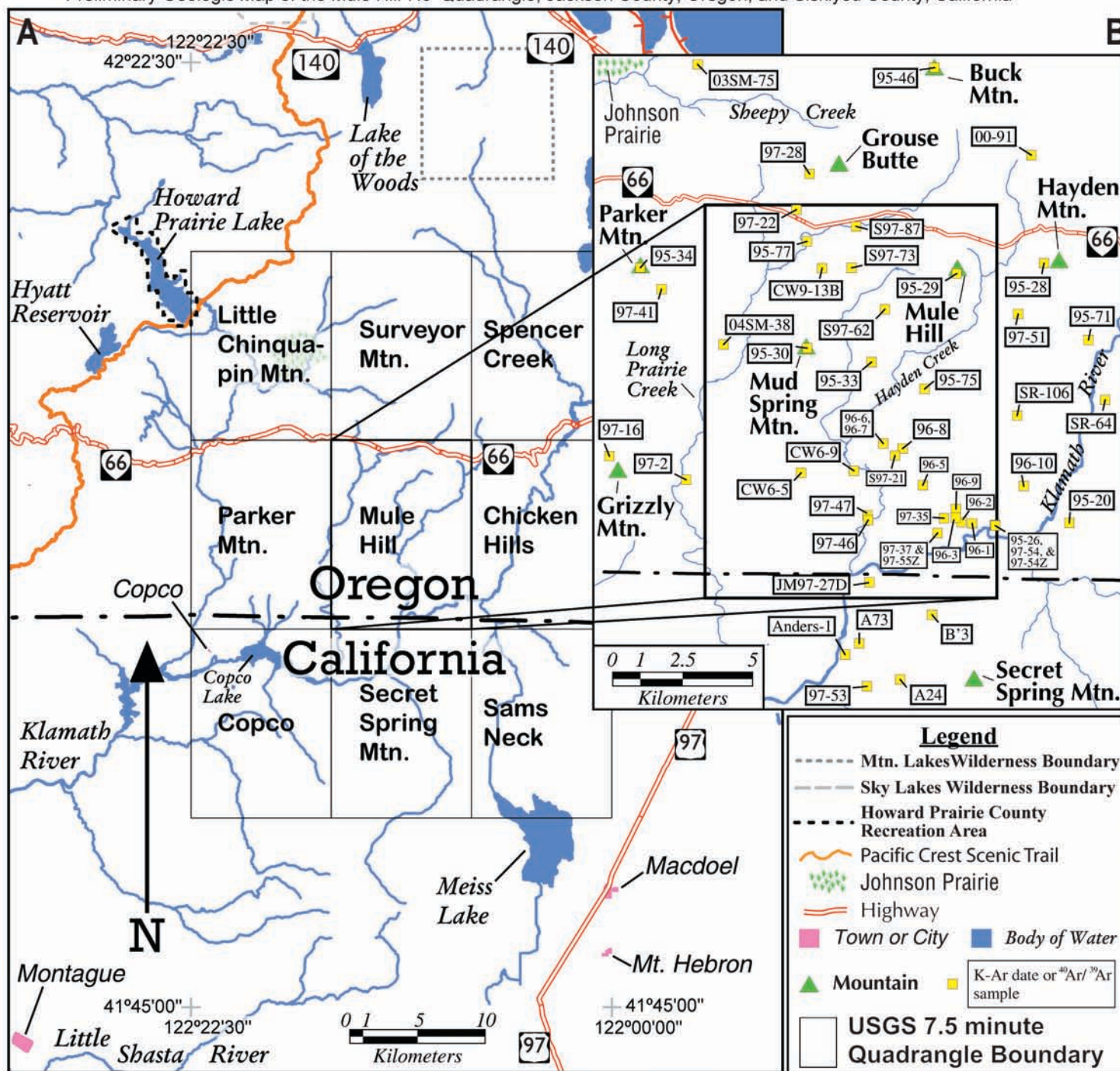


Figure 1. This series of location maps (A through D) provides a broad context in which to place the Preliminary Geologic Map of the Mule Hill 7.5' Quadrangle, Klamath County, Oregon, and Siskiyou County, California. Figures 1C and 1D were modified from U.S. Geological Survey (2006).

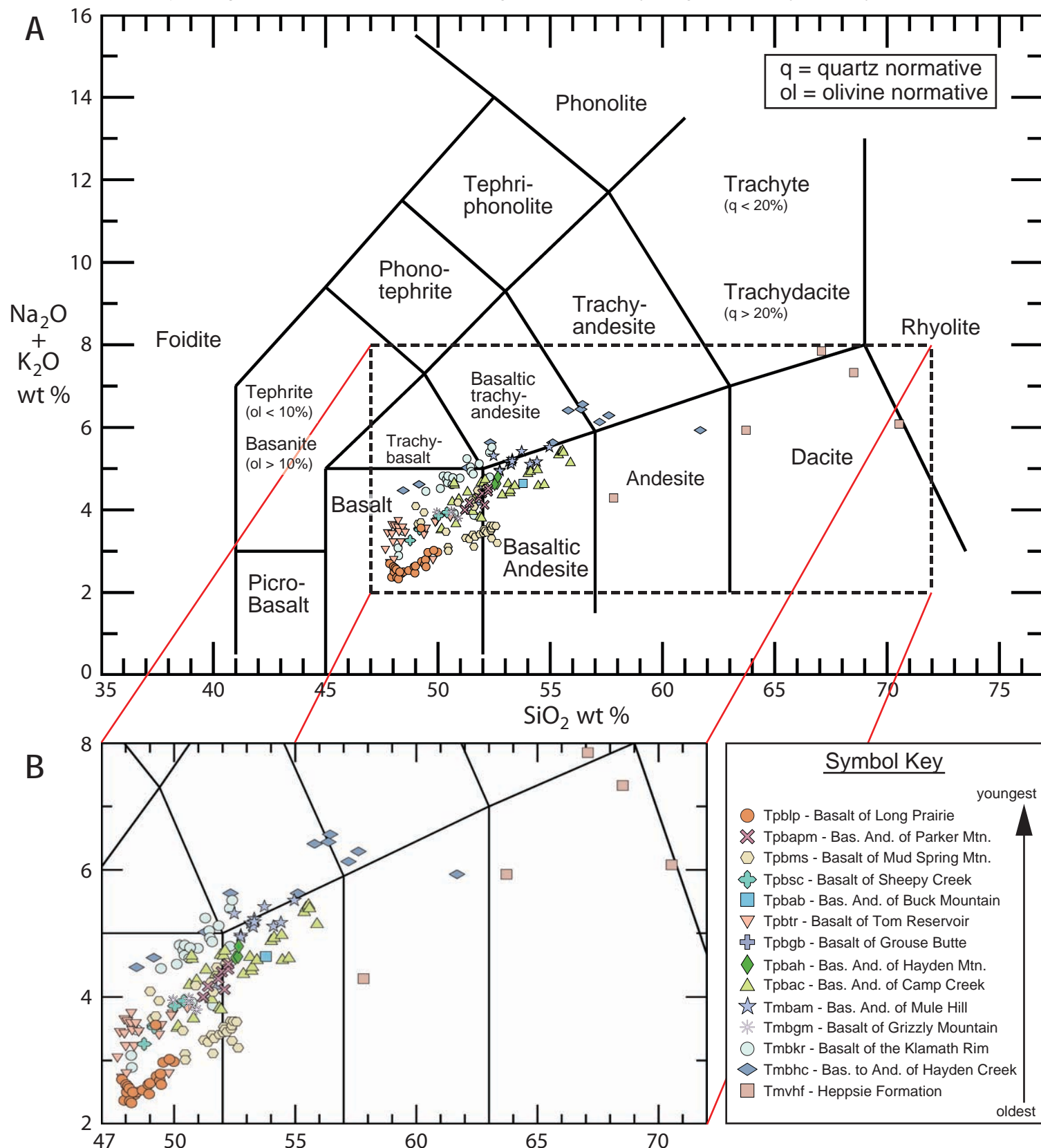


Figure 2. IUGS (International Union of Geological Sciences) classification system for volcanic rocks, which is based on total alkali (Na₂O + K₂O) vs. silica (SiO₂) content, with the superimposed data from analyzed Mule Hill quadrangle samples (except specimens collected on landslides [Qls unit] and including additional data from five Basalt of Grizzly Mountain [Tmbgm] samples collected within the Parker Mountain quadrangle; see Table 1) (Le Maitre, 2002).

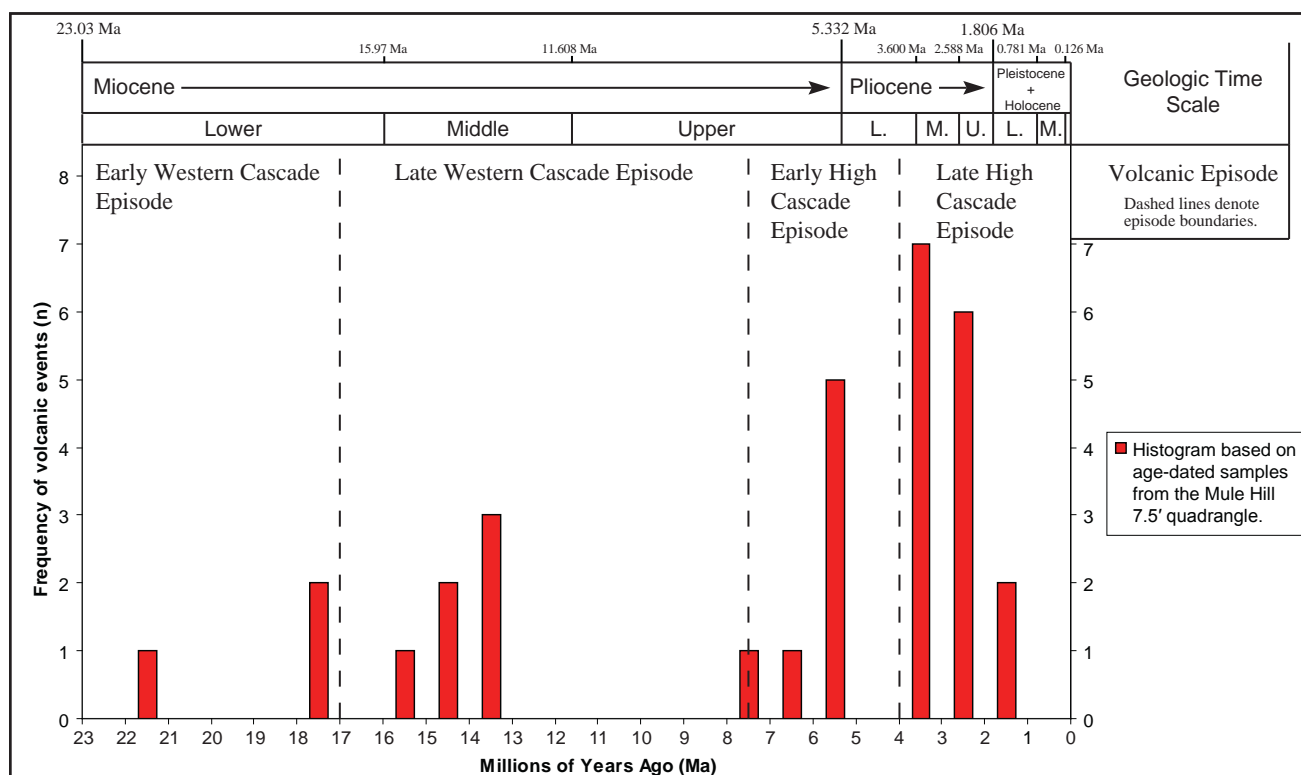


Figure 3. Histogram (number of samples with either a K/Ar or $^{40}\text{Ar}/^{39}\text{Ar}$ age date plotted as a function of geologic time in millions of years) of the geochronologic data derived from Mule Hill quadrangle samples.

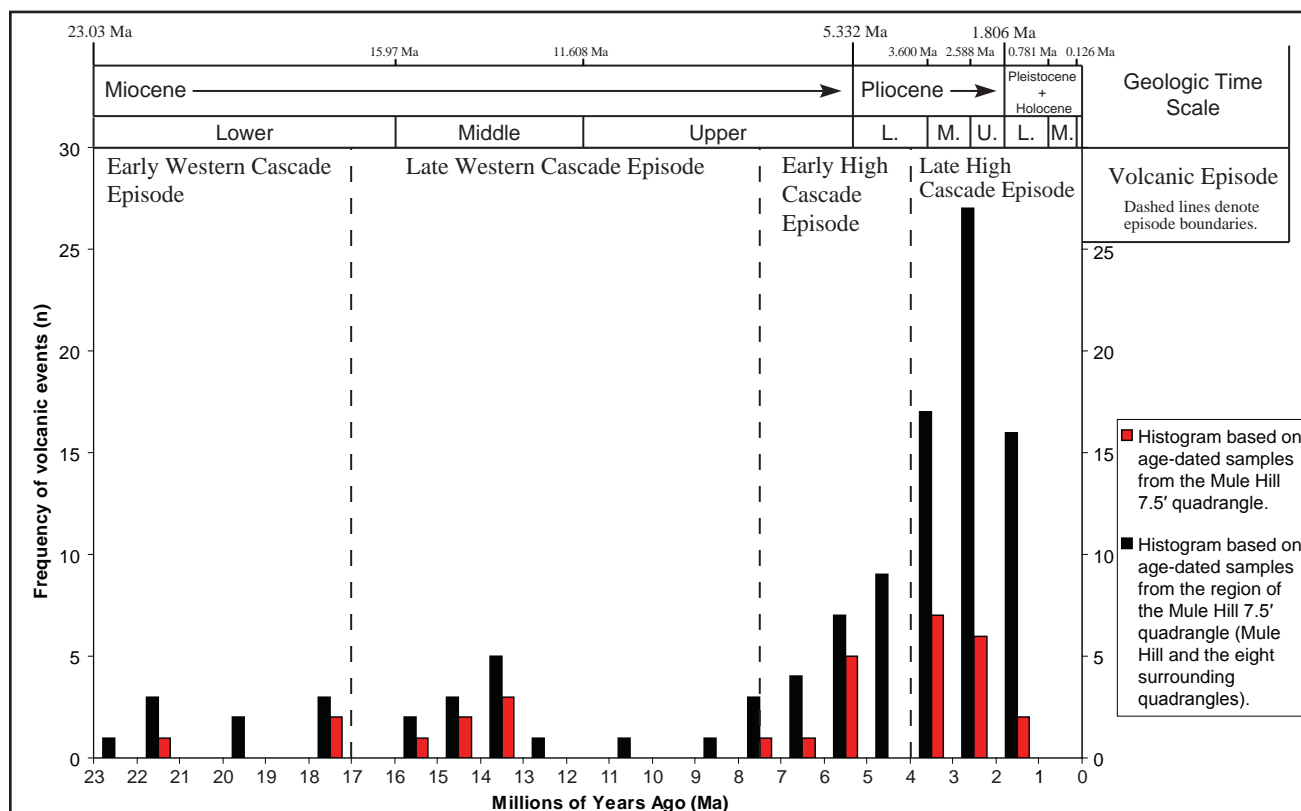


Figure 4. Histogram of the geochronologic data derived from Mule Hill quadrangle samples plus the eight surrounding quadrangles as well (see Figure 1).



Figure 5A. Kipuka of unusual 9 Ma hornblende andesite formed by a series of layers of lava flows and pyroclastics surrounded by younger volcanic rock that is located on the north side of Copco Reservoir (see Figure 1).

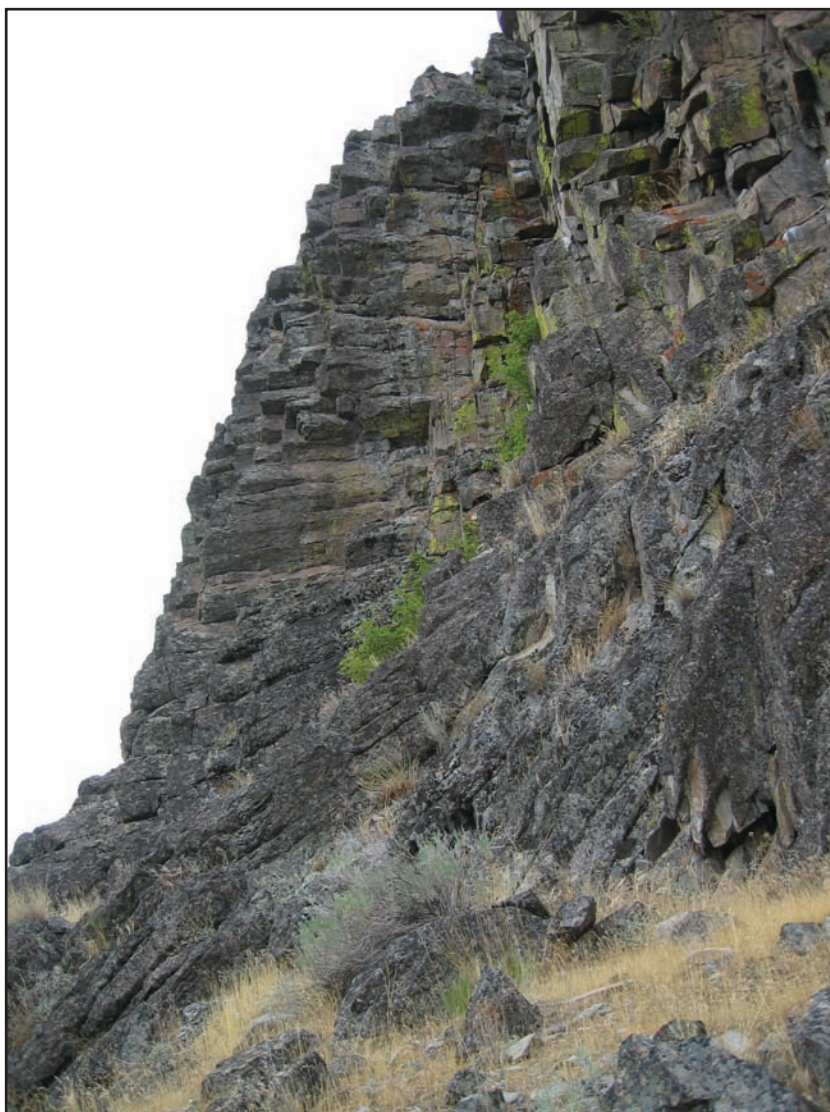


Figure 5B. On the far left side of the bluff depicted in Figure 5A is a dike of columnar jointed hornblende andesite that is 5 to 6 m wide with a chilled margin evident on the right side.



Figure 6A. Lava flows of the Basalt of the Klamath Rim (Tmbkr) with the oldest to the lower right and the youngest to the upper left. The slope depicted is on the north side of the Klamath River near the junction of the Mule Hill and Chicken Hills quadrangles. In this area 350 to 400 m of Tmbkr lavas are exposed (samples 08SM-61 through 65 are located at the 95-26 position on Figure 1 at higher stratigraphic levels).



Figure 6B. The base of the stratigraphic section of Tmbkr lavas is depicted (vehicle for scale). The arrows point to two light colored patches that are from the poorly welded pyroclastic material that constitutes the upper most segment of the Heppsie Formation (Tmvhf).



Figure 7A. This columnar jointed lava flow is the oldest Tmbkr lava flow and occurs at the very bottom of the stack of flows depicted in Figures 6A and B. The lava flow is 2 to 3 m thick; see the rock hammer for scale. Age dated sample 95-26 was collected from this particular outcrop.



Figure 7B. Beneath the lava flow depicted in Figure 7A is the top of the Heppsie Formation (Tmvhf). In much of the local area poorly welded pyroclastic flow material that aggregates 100 to 200 m in thickness constitutes the youngest portion of the Tmvhf. Pumice lumps 1 to 5 cm in diameter in a finer grained matrix of volcanic material that is poorly lithified make up the outcrop.



Figure 8. Located in the northeastern corner of the Mule Hill quadrangle is the Mule Hill basaltic andesite volcano. The picture was taken from a clear-cut on the north side of the volcano near Oregon state highway 66.

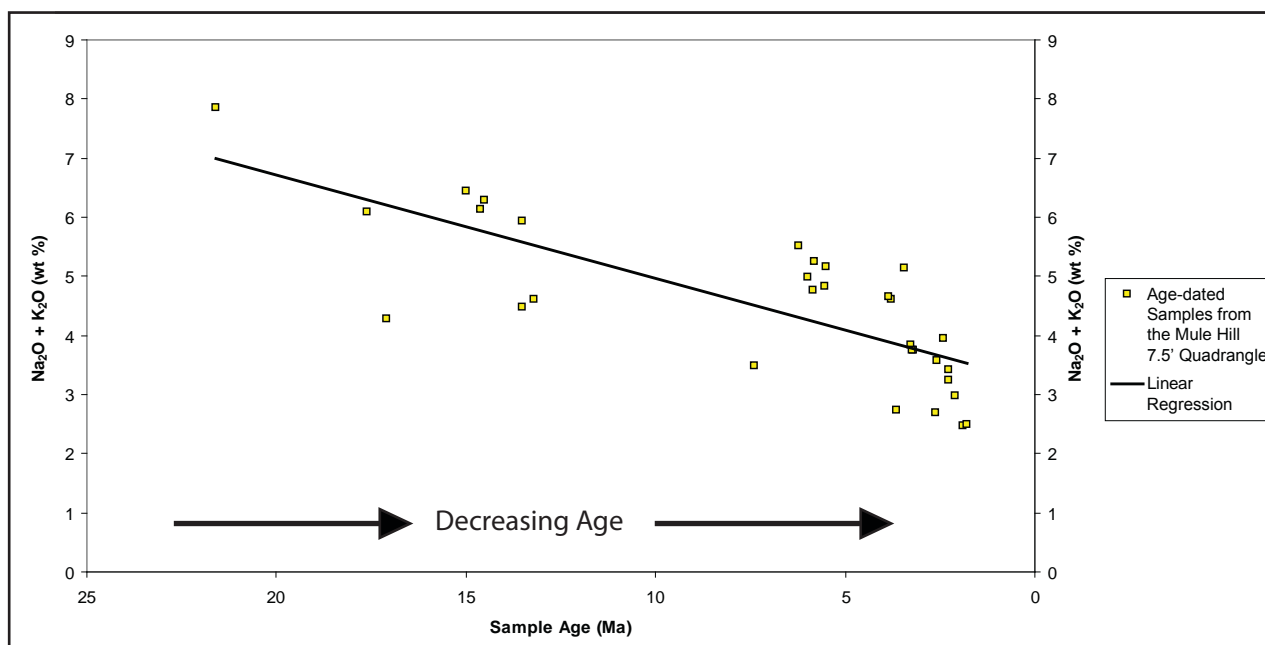


Figure 9. This plot of the alkali elements $\text{Na}_2\text{O} + \text{K}_2\text{O}$ versus age clearly portrays a pattern of declining $\text{Na}_2\text{O} + \text{K}_2\text{O}$ values as the rocks get younger. Since rocks become more mafic in terms of their color index (percent of ferromagnesian minerals present in an igneous rock hand sample [Philpotts, 1989]) as $\text{Na}_2\text{O} + \text{K}_2\text{O}$ decreases, the volcanic materials for which radiometric age dates have been determined, are becoming more mafic with declining age.

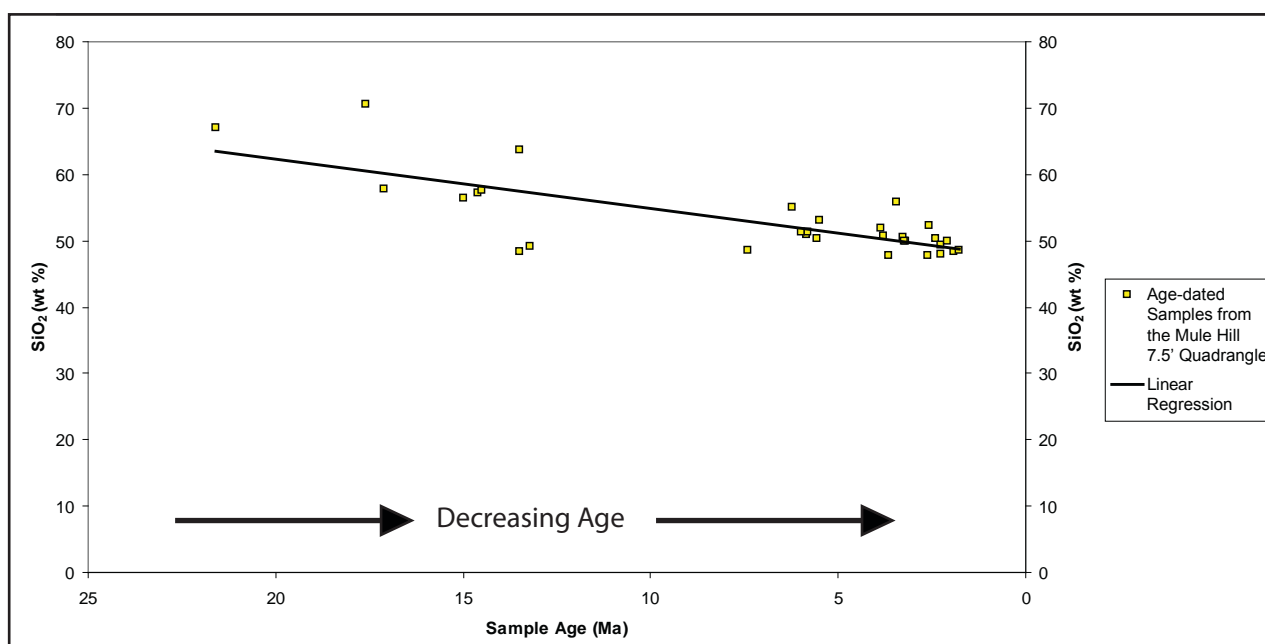


Figure 10. This plot of silica (SiO_2) versus age also portrays a clearly delineated chemical trend, in this case silica decreases with decreasing age. Since rocks become more mafic as the silica content decreases (moving from andesite to basaltic andesite to basalt [Philpotts, 1989; also see Figure 2]), the volcanic materials for which radiometric age dates have been determined are becoming more mafic with declining age.



Figure 11A. Looking south from the steep slope formed by Tmbkr lavas, Secret Spring Mountain forms the arcuate half-moon-like structure in the distance. The relatively flat, forested surface in the foreground is underlain by landslide material.

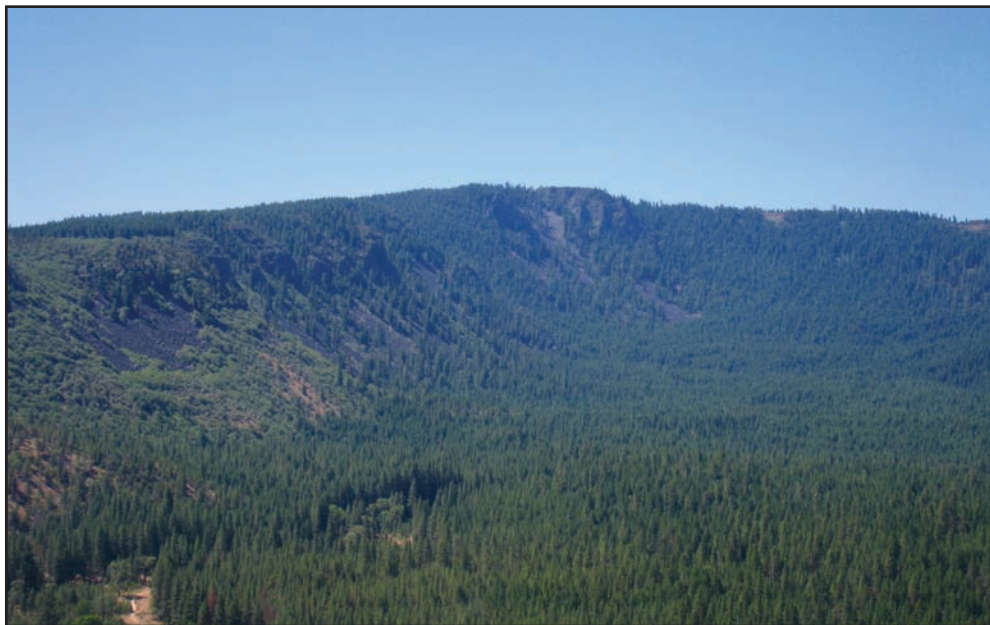


Figure 11B. The Secret Spring Mountain summit area consists of a plug-like mass (dike or dikes?) of non-vesicular aphanitic to finely granular igneous rock that is, in terms of its mineralogy and geochemistry, nearly identical to the lava flows that outcrop and are visible on the slope to the left of the conduit-forming rock. This rock mass provided the structural strength to form the headwall of the massive landslide you see in the foreground of Figure 11A.



Figure 11C. This view of the Klamath River canyon, taken from the same vantage point as 11B, depicts what happens to the river once it begins to cut down through the landslide debris. Both above and below the Secret Spring landslide the Klamath River is a much more placid river in terms of its everyday flow characteristics. Hell's Corner is the name given to the class IV+ rapids seen in the photo.



Figure 11D. Several rafts are clearly visible coming down the Klamath River Canyon and going through Hell's Corner.

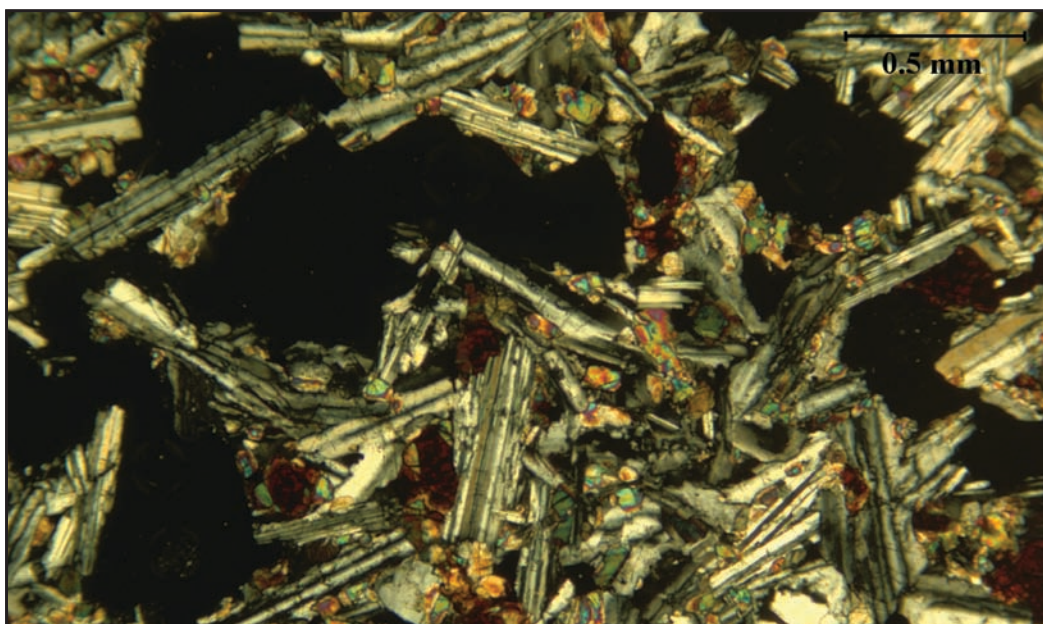


Figure 12. This photomicrograph is from a thin section of a Basalt of Long Prairie (Tpblp) sample, taken under crossed polarizer conditions. The image depicts the diktytaxitic texture so characteristic of this unit. The black voids in the photomicrograph are vesicles, holes created by the effervescence of the volcanic gases H_2O and CO_2 as the lava was extruded onto the Earth's surface. The thin rectangular crystals that project into the vesicles and have gray to white "stripes" are twinned plagioclase feldspar crystals.

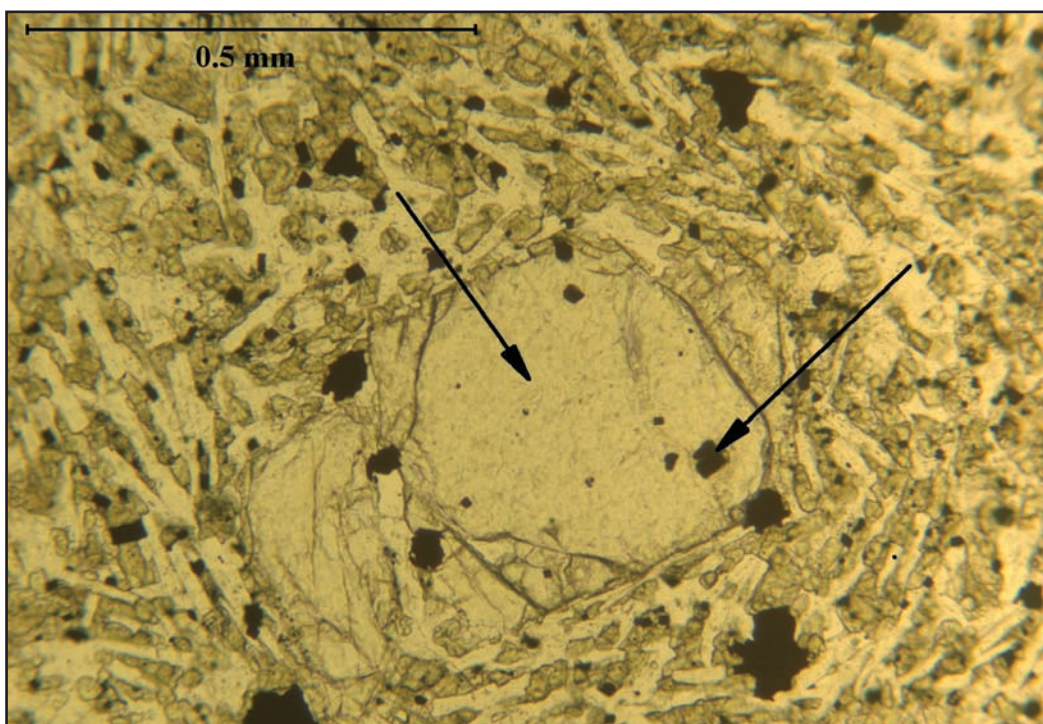


Figure 13. This photomicrograph is from a thin section of a Basalt of Long Prairie (Tpblp) sample, taken under uncrossed polarizer conditions. The left hand arrow indicates an olivine phenocryst and the right hand arrow points out one of a number of included early-formed crystals of spinel enclosed within the later crystallizing olivine grain.

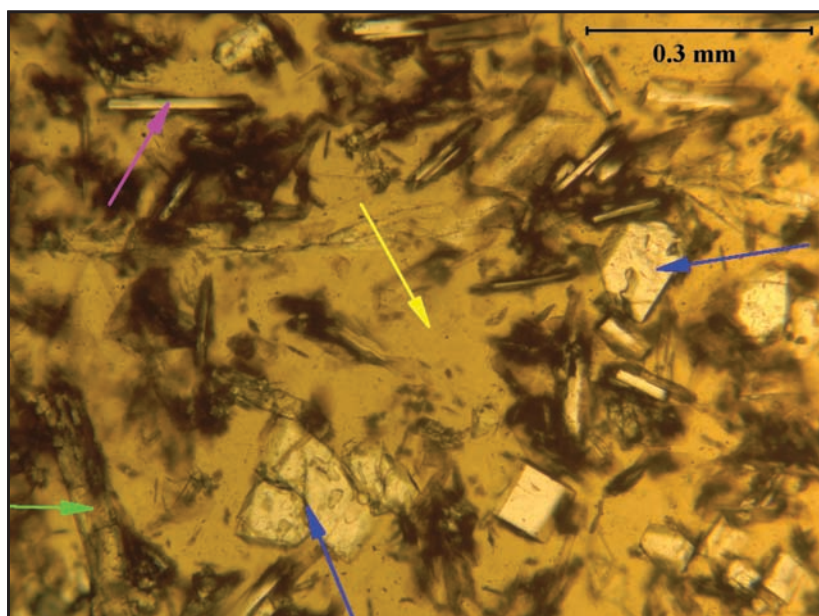


Figure 14A. This photomicrograph, taken with the polarizers not crossed, shows an intersertal texture in which the cooling has been so sudden that basalt glass has been preserved. The centrally located arrow points out the brownish colored glass. Both the right hand arrow and the center bottom arrow indicate olivine crystals; the upper left hand arrow points out a plagioclase feldspar crystal while the arrow to the lower left hand corner of the photo indicates a clinopyroxene crystal.

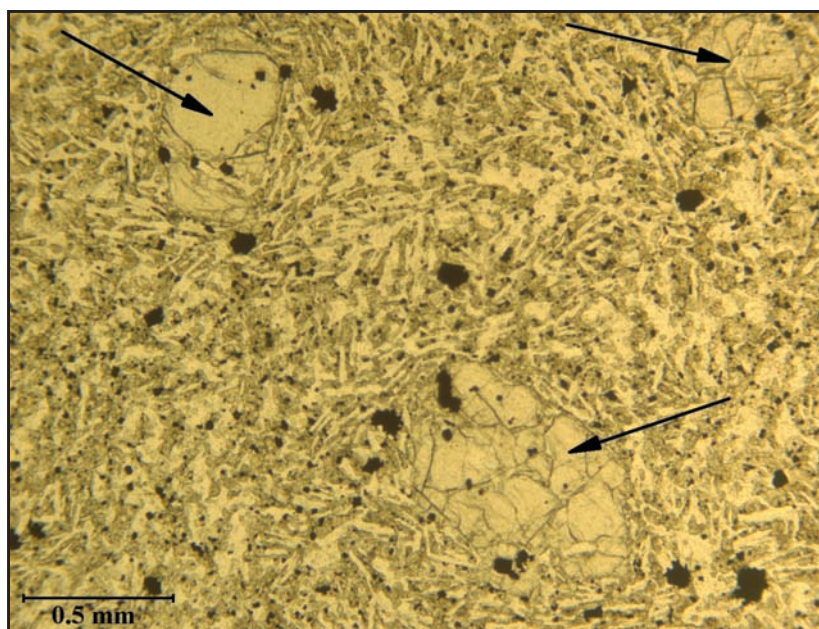


Figure 14B. This photomicrograph taken with uncrossed polarizers, depicts an intergranular texture with three arrows pointing out olivine phenocrysts, each with small included grains of spinel. Surrounding the olivine crystals are small grains of light colored plagioclase feldspar and equally small grains of colored clinopyroxene and whitish colored olivine together with black opaque grains of titanomagnetite. An intergranular texture results from a slower rate of cooling than an intersertal texture.

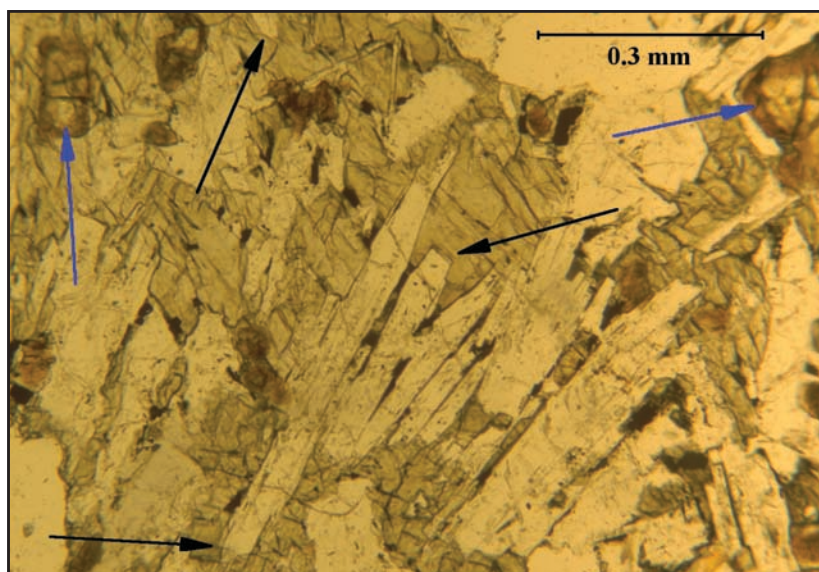


Figure 14C. This photomicrograph taken with uncrossed polarizers, demonstrates a subophitic texture. This texture is more coarse-grained due to a slower rate of cooling that provides more time for the crystals to grow to a larger size. The arrows in the far left and far right corners of the photomicrograph delineate olivine crystals, which have been partially altered through oxidation and hydration chemical reactions to iddingsite. The three remaining arrows point out locales where clinopyroxene has grown around the terminations or ends of plagioclase feldspar crystals, the key ingredient to recognizing a subophitic texture.



Figure 15A. Chemical and mechanical weathering of Mud Spring Mountain lava flows typically develop elliptically to spherically shaped boulders.



Figure 15B. Continued lava flow movement down hill under the influence of gravity has stretched vesicles out in a direction parallel to flow movement.

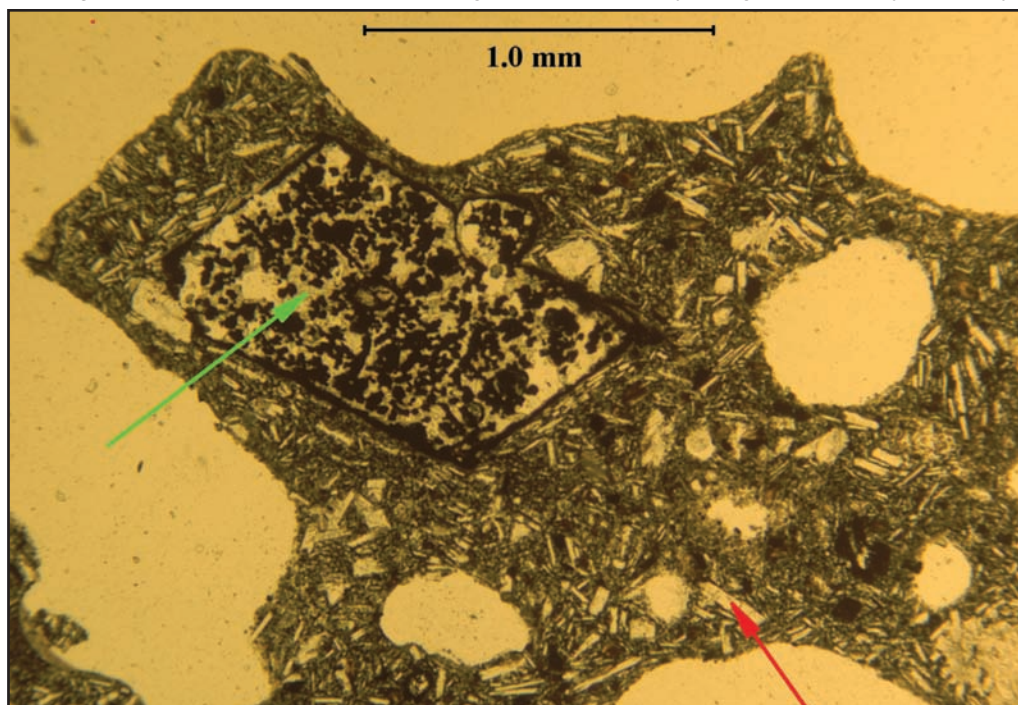


Figure 16A. This photomicrograph taken with uncrossed polarizers shows an olivine phenocryst (left arrow) that exhibits severe high temperature oxidation (Haggerty and Baker, 1967). Olivine, when exposed to O_2 bearing vapors / fluids at high temperature, breaks down to a magnesian orthopyroxene and an Fe^{+3} -rich oxide phase. The arrow to the lower right side delineates a rectangular shaped plagioclase feldspar, the mineral most abundant in the matrix of the Mud Spring Mountain lavas. The large white areas, some of which are elliptical to spherical in shape, are vesicles.

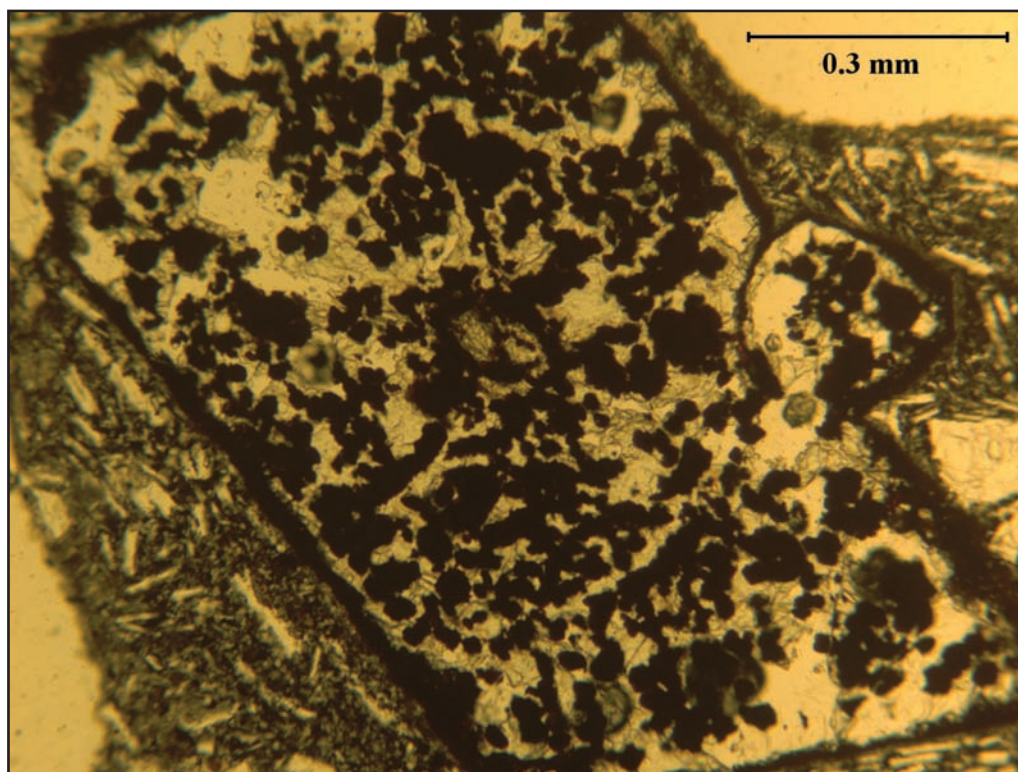


Figure 16B. This photomicrograph focuses on the texture of the altered olivine phenocryst shown in Figure 16A. The sheer number of exsolving opaque Fe^{+3} -rich grains is quite impressive.

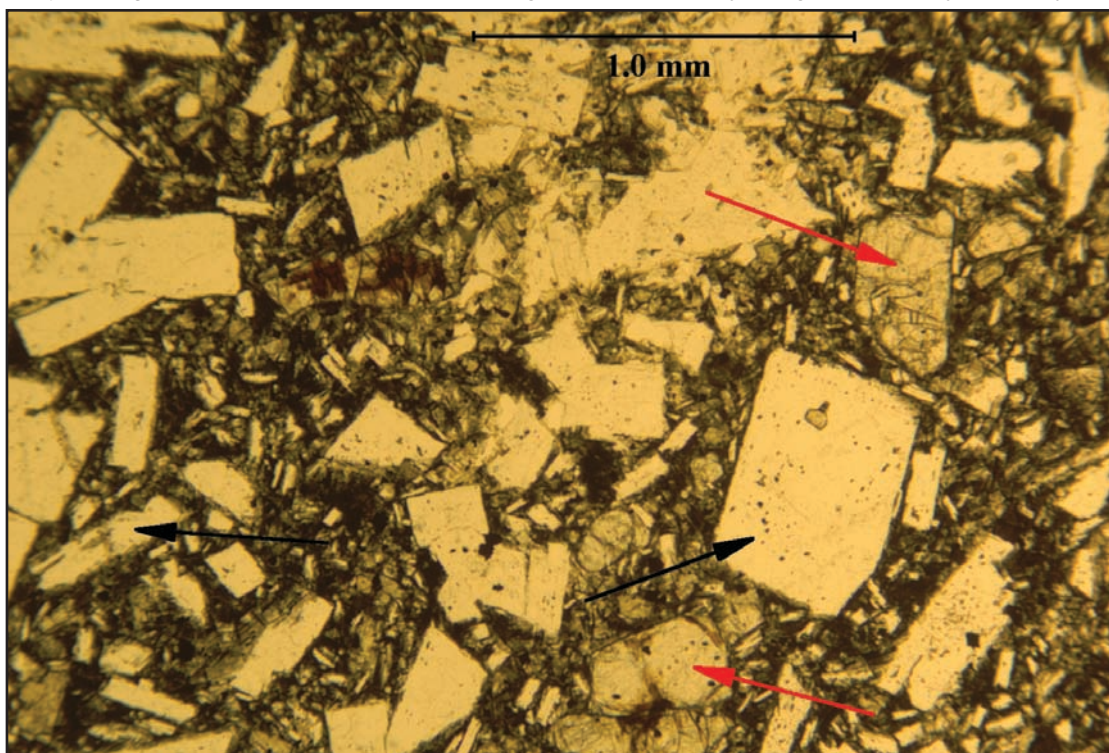


Figure 17A. This photomicrograph taken with uncrossed polarizers is of the Basaltic Andesite of Mule Hill, specifically from a sample collected quite near a vent at the top of the mountain. Notice the abundance of plagioclase feldspar phenocrysts as pointed out by the two black arrows. The crystal shapes can vary from blocky to a more elongate rectangular habit. The two red arrows indicate small olivine phenocrysts that constitute only several percent of the typical Mule Hill lava. The matrix is intersertal in texture and is quite dark due to finely disseminated opaque iron oxide minerals.

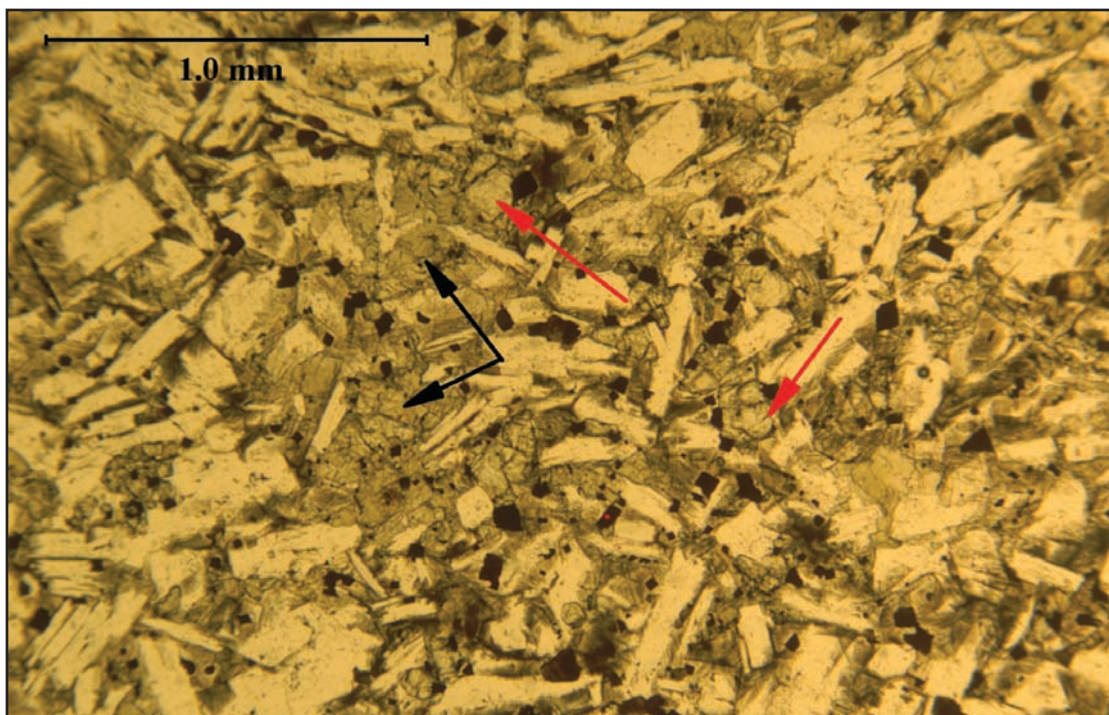


Figure 17B. This photomicrograph is from a Mule Hill lava flow sample wherein the black arrows are indicating the second most abundant mineral after plagioclase feldspar; namely, clinopyroxene. The two red arrows point out small olivine crystals that are lighter in color than the clinopyroxene and are marginally altered to iddingsite, brown in color, which is a low temperature secondary mineral formed as a result of oxidation and hydration chemical reactions (Baker and Haggerty, 1976).

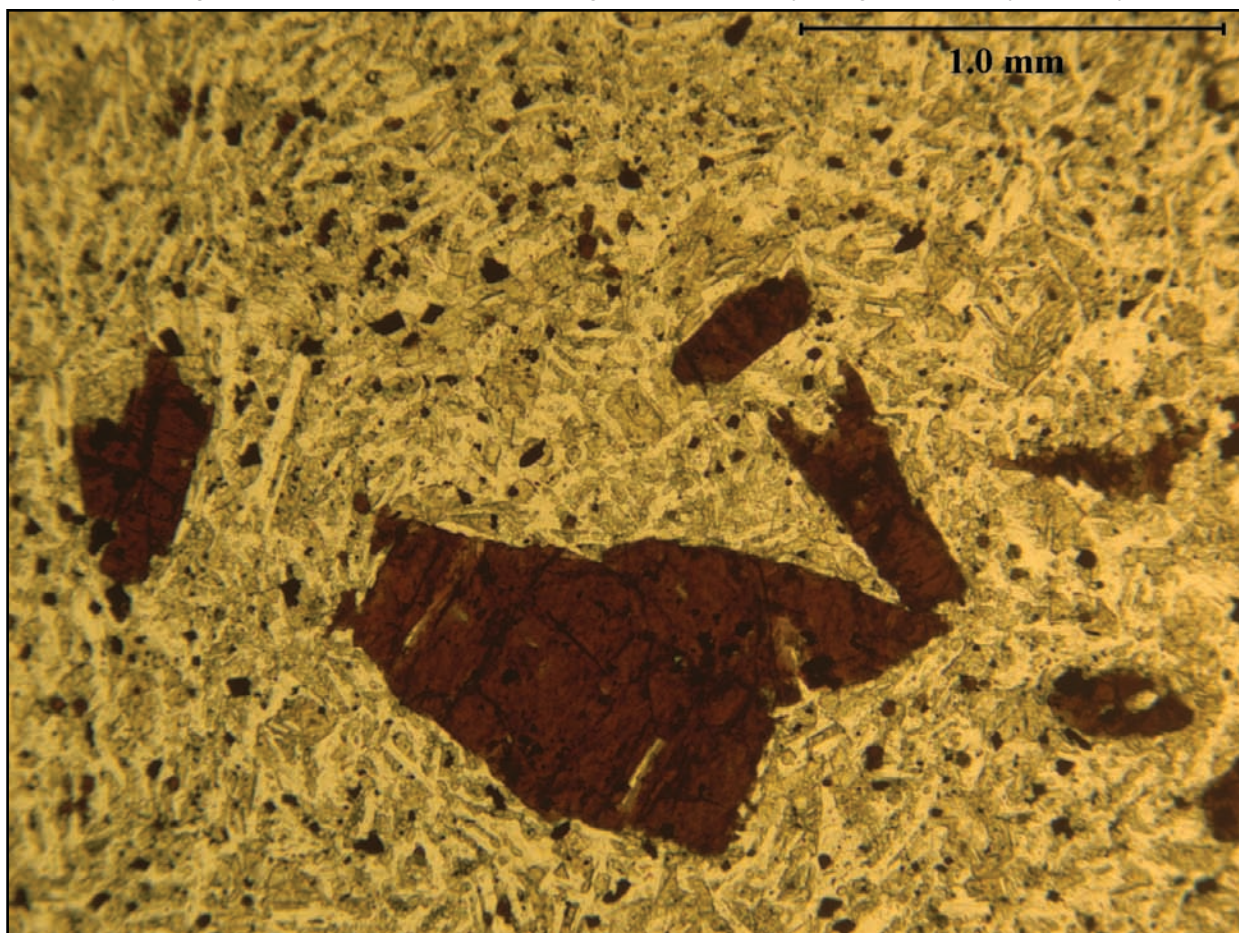


Figure 18. This photomicrograph is from a lava of the Basalt of Grizzly Mountain. The olivine phenocrysts have been completely altered to iddingsite, yet clinopyroxene and plagioclase feldspar that completely dominate the matrix are both free from alteration. This photo demonstrates the unstable nature of olivine under oxidizing conditions well below the solidus temperature of the lava.

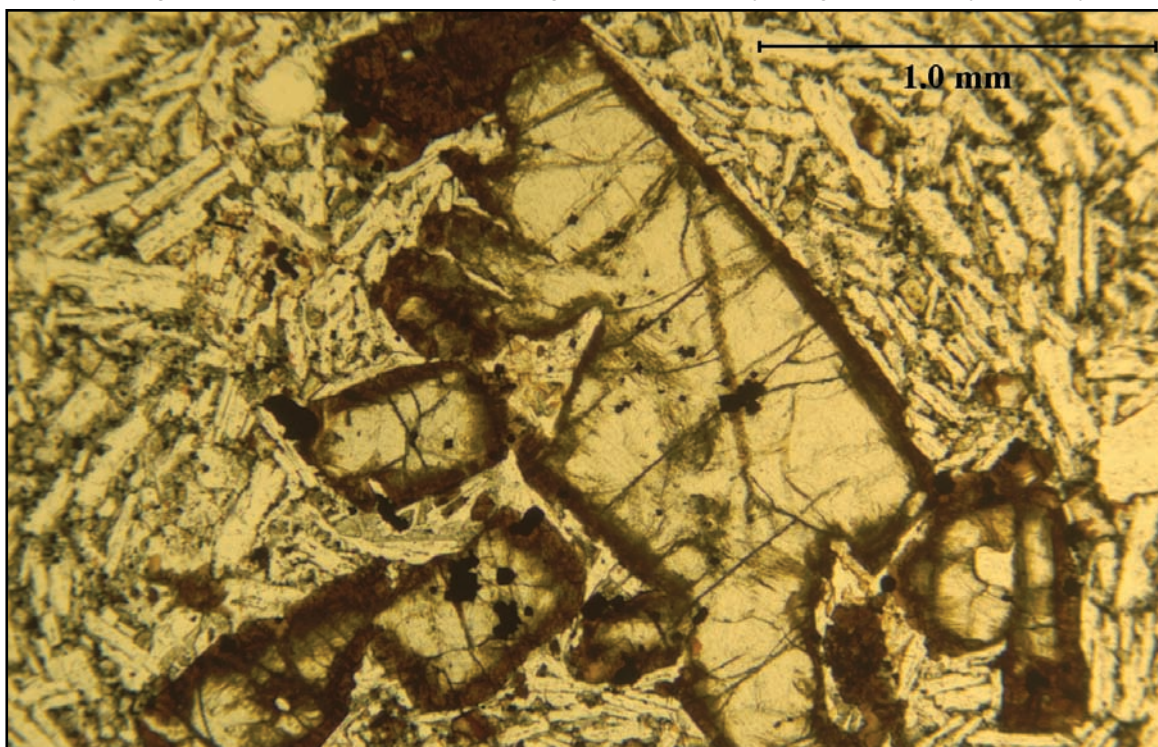


Figure 19A. Basalt of the Klamath Rim (Tmbkr) characteristically has glomeroporphyritic clumps of olivine phenocrysts as depicted in this photomicrograph, which was taken with uncrossed polarizers. The olivine crystals are completely rimmed with iddingsite, which armors them and slows down the rate at which the alteration process can proceed.

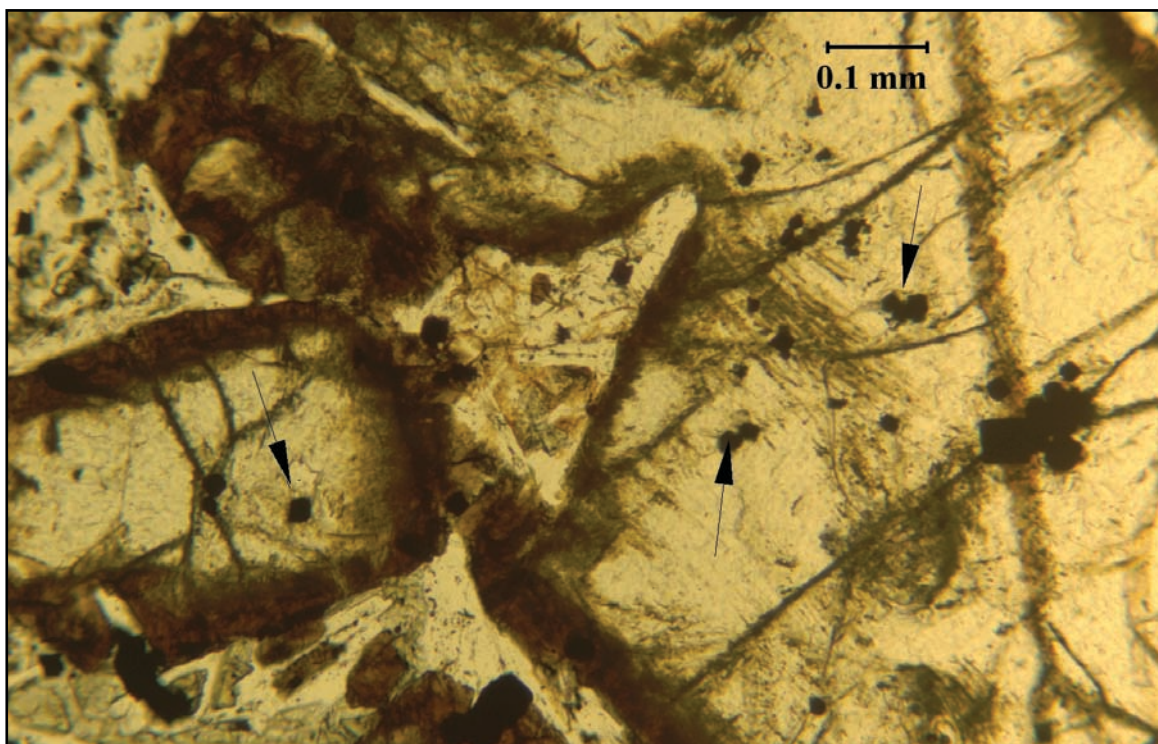


Figure 19B. Under higher magnification the early formed spinel crystals that occur on the inside of the olivine phenocrysts become more noticeable. The poikilitic texture clearly indicates that the spinel mineral crystallized first and the olivine sometime later and enveloped the spinel.

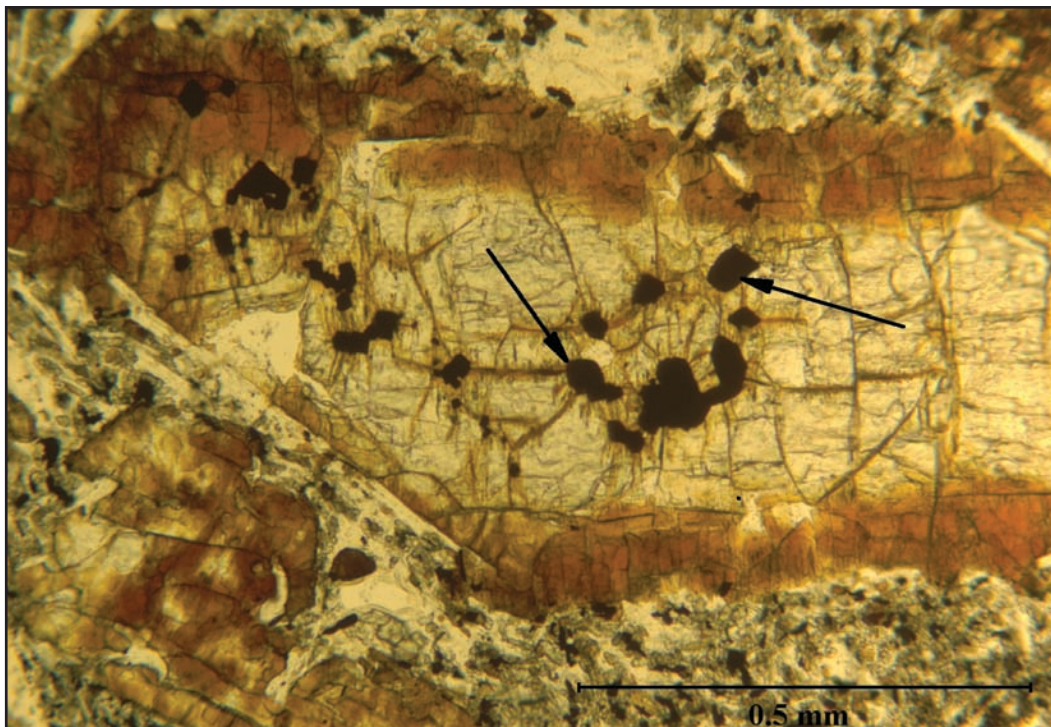


Figure 20. Olivine phenocrysts from the Basalt to Andesite of Hayden Creek (Tmbhc) are marginally altered to iddingsite that penetrates further into the olivine than is depicted in Figures 19A and B. Primary olivine still survives in the interior of the phenocrysts along with a number of poikilitically enclosed early-formed spinel crystals.

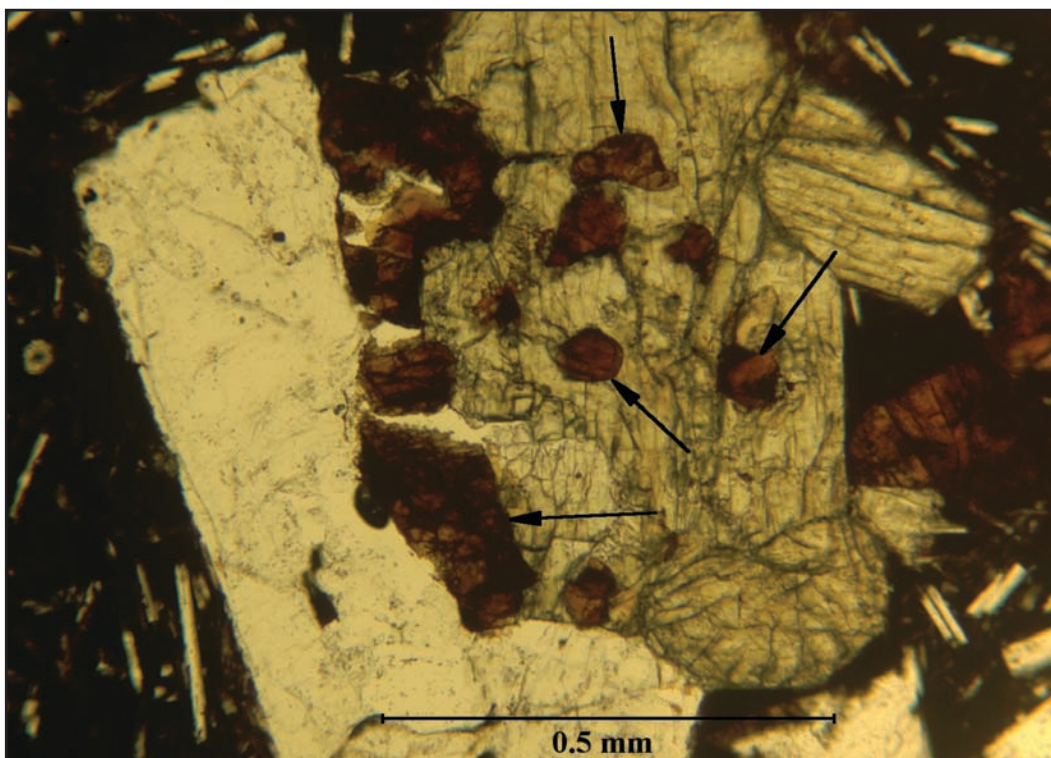


Figure 21. This photomicrograph is from a more siliceous lava flow from the Basalt to Andesite of Hayden Creek. In this case notice the four small olivine crystals that are indicated by arrows are completely altered to iddingsite while the closely juxtaposed clinopyroxene crystal and the large white rectangular plagioclase crystal are pristine, with no hint of chemical alteration.

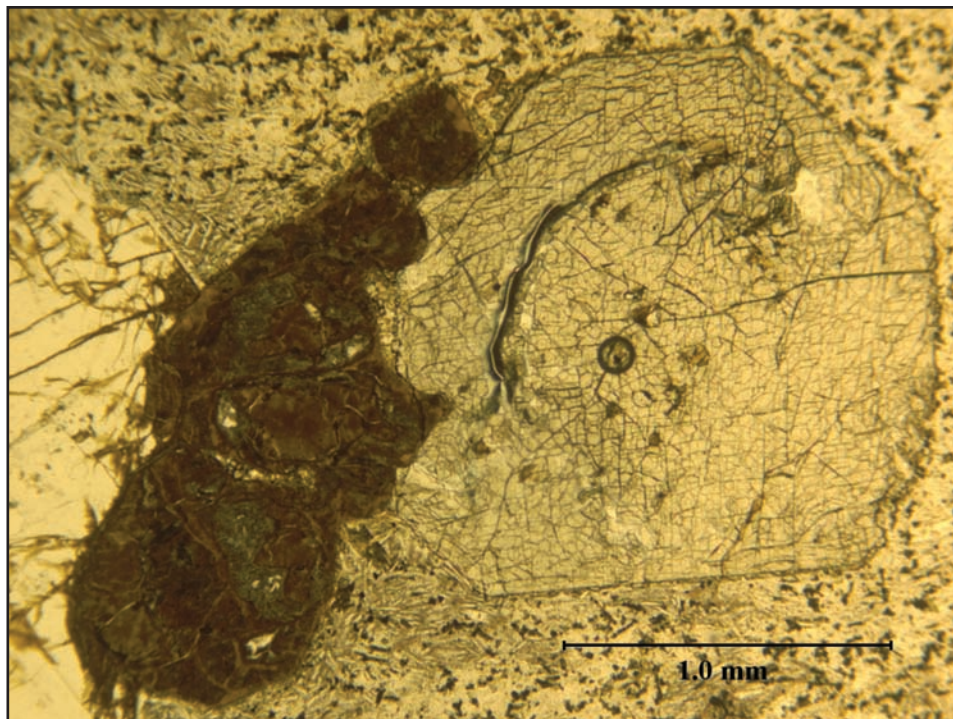


Figure 22A. From left to right are a larger phenocryst of plagioclase feldspar, an olivine phenocryst that has been completely converted to iddingsite, and a large clinopyroxene phenocryst that demonstrates two cleavage directions intersecting at a nearly 90° angle, one of the salient physical characteristics of the pyroxene family of minerals. This photomicrograph is from a rather typical Heppsie Formation basaltic lava and was taken under uncrossed polarizers.

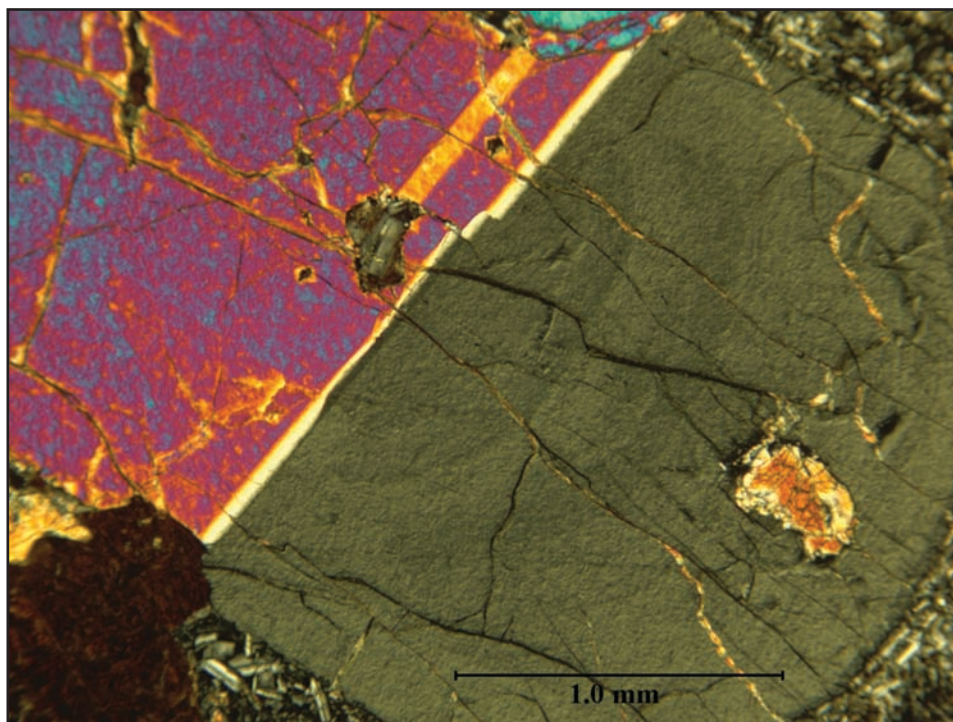


Figure 22B. Focusing on the clinopyroxene phenocryst under higher magnification and with the polarizers crossed, an albite twin crosses the clinopyroxene crystal from lower left to upper right. The twin has several fault-like fractures that offset the twin plane. Notice the darker concentric bands in the darker segment of the phenocryst to the lower right of the photo. These bands reflect changing chemical composition within the clinopyroxene and that chemical equilibrium between the crystal and the surrounding magma could not be maintained.

Table 1 (page 1). Whole rock chemical data and potassium-argon (K-Ar) ages (^a indicates an argon-argon age) for the samples from the Preliminary Geologic Map of the Mule Hill 7.5' Quadrangle, Klamath County, Oregon, and Siskiyou County, California. The major element oxides are presented in weight percent and the trace elements are reported in parts per million (ppm). The chemical data are X-ray fluorescence (XRF) results and were measured in the X-ray laboratory of the Department of Earth and Environment, Franklin and Marshall College, Lancaster, Pennsylvania. The UTM coordinate values are according to the UTM Zone 10 (NAD 27 for US) projection. All UTM coordinates have been rounded to the nearest 10 m. The 1/4 of 1/4, Section (Sec.), Township (T.), and Range (R.) columns are location descriptors of the Public Land Survey System (PLSS) (Willamette meridian and base line [except for the samples denoted by ^{CA} that were collected in California: Mt. Diablo meridian and base line]). In the Lithology column (Lith.), B = basalt (SiO₂ = 45-52%), BA = basaltic andesite (SiO₂ = 52-57%), A = andesite (SiO₂ = 57-63%), D = dacite (SiO₂ = 63-74%), TrB = trachybasalt, BTrA = basaltic trachyandesite, TrA = trachyandesite, and Tr = trachyte (consult Figure 2 of this report). See Figure 2 and Le Maitre (2002) for details regarding lithological classification. Please consult the detailed descriptions in this report or the geologic map for the full unit names. This table is 4 pages long.

Map no.	Sample no.	K-Ar Age ^a	1/4	1/4 Sec.	T. R.	UTM E	UTM N	Unit	Lith.	SiO ₂	TiO ₂	Al ₂ O ₃	Fe ₂ O ₃	FeO	MnO	MgO	CaO	Na ₂ O	K ₂ O	P ₂ O ₅	LOI (%)	Total Fe ₂ O ₃ T	Rb	Sr	Y	Zr	V	Ni	Cr	Nb	Ga	Cu	Zn	Co	Ba	La	Ce	U	Th	Sc	Pb	Yb	Be			
	97-54Z	17.1±0.8	NW	NW	9	41	6	572390	4652490	Tmbrh	A	57.82	1.09	15.64	4.41	2.04	0.14	2.56	5.08	2.84	1.45	0.48	7.10	100.65	6.68	23.3	462	27.7	162	108	6	26	9.1	19	23	88	10.5	704	22.3	50.8	1.1	3.5	20	9.7	--	--
	97-54	13.5±0.5	NW	NW	9	41	6	572390	4652490	Tmbrh	A	63.72	0.89	14.86	3.41	1.36	0.12	1.14	2.64	2.91	3.02	0.19	6.46	100.52	4.92	43.9	266	33	262	63	16	29	10.9	19.4	19	70	12	782	27	55	2.9	8.4	16	9.9	--	--
	97-37	21.6±0.5	SE	NE	7	41	6	570340	4652200	Tmbrh	Tr	67.08	0.81	15.82	3.20	1.04	0.06	0.56	2.44	2.15	0.20	2.08	100.28	3.46	29.5	353	39	263	49	4	11	11.5	20.5	8	93	4	760	30	59	2.8	7.8	13	9.9	--	--	
	97-55Z	17.6±0.7	SE	NE	7	41	6	570340	4652200	Tmbrh	D	70.54	0.70	13.00	3.69	0.21	0.06	0.50	2.30	4.26	1.82	0.22	2.99	100.29	3.92	24.2	297	28.4	208	45	4.6	21	10.5	17.9	17	72	4.5	633	23.4	49.3	1.6	5.1	13	11.6	--	--
	97-36	--	SE	NE	7	41	6	570340	4652200	Tmbrh	D	68.52	0.72	14.89	2.61	0.26	0.09	0.43	2.25	5.11	2.22	0.25	2.28	99.63	2.90	35.8	289	46.2	253	37	2.2	11	12.8	18.4	6	88	4.1	728	32.8	68	1.8	6	14.6	11	--	--
	96-6	13.5±0.4	SE	NE	36	40	5	568380	4653500	Tmbrh	B	48.45	1.79	15.45	4.88	6.29	0.16	7.80	8.27	3.25	1.22	0.59	1.50	99.65	11.87	17.8	637	42	148	242	178	370	10.4	22.3	64	106	49	530	24	47	2.3	3.8	25	5.7	--	--
	96-8	13.2±0.3	SW	NW	31	40	5	569070	4655170	Tmbrh	B	49.16	1.82	16.14	4.61	6.41	0.16	6.49	8.55	3.40	1.22	0.74	99.26	11.73	16.8	667	29	149	251	115	21	11.6	21.7	59	101	41	556	19	50	1.1	5.6	26	4.9	--	--	
	CW6-9	15.0±0.4	SW	SW	36	40	5	567350	4654370	Tmbrh	BTrA/TrA	56.37	1.73	15.97	4.95	4.57	0.16	2.36	5.55	4.77	1.67	0.78	100.28	10.03	23.4	526	146	157	212	5	15	4.3	23.8	33	93	15	725	56	58	1.2	5.7	26	8.4	--	--	
	S97-21	14.6±0.9	NW	SW	31	40	5	568800	4654920	Tmbrh	TrA	57.20	1.29	16.37	4.72	3.00	0.12	2.49	5.51	3.66	2.47	0.46	2.33	99.62	8.05	42.9	519	40	273	172	18.8	36	12.3	20.6	66	93	11.7	769	33.8	57.9	1.3	5.2	20	13.4	--	--
	96-7	14.5±0.5	SE	NE	36	40	5	568380	4653500	Tmbrh	TrA	57.61	1.33	16.86	5.94	2.22	0.13	2.17	5.31	3.93	2.36	0.45	1.85	100.16	8.41	40	500	44	266	176	30	41	10.4	22.3	60	90	18	787	28	57	1.9	7.5	20	8.4	--	--
	S97-91	--	SE	SE	25	40	5	568380	4653500	Tmbrh	TrB	51.30	1.24	17.80	4.54	5.34	0.16	5.05	8.08	3.81	1.21	0.59	1.21	100.33	10.47	9.6	835	26.9	124	208	70	106	9.8	20.2	79	94	26	588	18.2	53.9	0.6	2	23.2	8.9	--	--
	S97-19	--	SE	NE	36	40	5	568350	4653270	Tmbrh	BTrA	52.33	1.25	17.61	3.08	6.17	0.17	4.78	7.51	4.14	1.49	0.74	0.75	100.02	9.94	11.2	774	23.2	165	187	48	71	11.8	20.3	73	94	28	614	24.2	58.7	0.9	3.5	21.8	8.6	--	--
	S97-20	--	SE	NE	36	40	5	568240	4652200	Tmbrh	BTrA	55.11	1.14	17.10	6.18	2.21	0.13	4.34	6.71	4.09	1.54	0.30	1.62	100.47	8.64	21.6	643	20.9	154	172	63	131	7.1	20.7	50	75	20	544	13.7	41.5	1.5	5	21	12.3	--	--
	S97-35	--	NE	NE	1	41	5	568390	4653870	Tmbrh	BTrA	56.80	1.68	15.81	5.16	4.40	0.25	2.88	6.03	4.84	1.57	0.76	100.10	10.02	23.5	530	36	152	239	4	17	8.9	21.7	41	99	15	646	21.7	48.6	1.2	3.8	27	10.1	--	--	
	S97-31	--	SE	SW	36	40	5	567530	4654590	Tmbrh	TrA	56.44	1.68	15.74	4.57	4.37	0.17	2.79	5.92	4.93	1.63	0.76	100.18	9.43	23.7	518	34	159	236	4	14	8.9	21.7	41	99	15	602	22.4	55.9	1.2	4.1	27.2	11.7	--	--	
	JM97-18 ^{CA}	--	SE	NE	13	48	3	570200	4650250	Tmbrh	A	61.68	0.66	17.01	3.69	1.02	0.06	1.69	4.53	3.60	2.33	0.22	0.39	96.88	5.24	53	655	20	211	93	10	22	9	18	13	62	12	566	22	47	2	10	--	--	--	
	95-26	7.41±0.19	NW	NW	9	41	6	572380	4652510	Tmbrh	B	48.27	1.32	17.30	2.54	8.00	0.17	7.96	8.57	3.77	0.87	0.46	0.95	99.82	11.43	7.1	439	24.3	83	263	131	247	6.8	18.4	91	88	39	307	11.6	23.3	0.3	0.8	31.5	6.5	--	--
	96-3	5.55±0.18	SE	SW	5	41	6	570980	4652750	Tmbrh	B	50.23	1.24	17.00	5.54	4.53	0.16	5.79	8.86	3.75	1.01	0.35	1.06	99.58	10.57	9.8	924	25	102	226	90	99	8.4	21.9	85	77	29	535	17	44	2.3	6.3	22	4.7	--	--
	JM97-27 ^{CA}	5.63±0.15	SE	NW	14	48	3	567940	4650440	Tmbrh	B	50.98	1.26	17.35	2.74	6.73	0.17	5.30	3.61	1.16	0.62	1.01	99.16	10.22	10.3	747	23.1	131	201	101	99	16.2	20.6	75	91	28.4	550	19.1	57.5	0.6	2.1	25	8.8	--	--	
	96-5	5.8±0.2	NW	NE	6	41	6	568810	4654890	Tmbrh	TrB	51.29	1.33	18.20	7.47	2.94	0.17	3.65	7.72	4.04	1.20	0.75	1.08	99.84	10.74	5.9	818	30	163	196	55	98	11.2	23.1	45	99	30	763	28	62	1.1	4.5	21	7.5	--	--
	JM97-48 ^{CA}	--	SE	NW	13	48	3	569370	4650250	Tmbrh	B	48.23	1.25	17.20	8.05	2.89	0.17	7.00	11.03	2.65	4.03	0.26	0.37	99.23	11.26	3	520	24	80	272	302	5	18	69	76	49	443	13	38	1	2	--	--	--	--	
	JM97-27 ^{CA}	--	SE	NW	14	48	3	567940	4650440	Tmbrh	B	48.25	0.96	17.21	2.22	7.34	0.16	9.37	11.63	2.63	0.26	0.17	0.36	100.58	10.38	2	285	25	51	292	123	190	3	17	154	63	42	122	3	9	--	--	--	--		
	S97-29	--	SW	NE	1	41	5	568010	4653480	Tmbrh	B	49.24	1.00	18.43	3.74	5.51	0.16	7.41	10.10	3.27	0.29	0.19	0.96	100.30	9.86	3.2	535	19.1	63	187	138	188	4.2	17.9	69	66	36	225	6.7	20.2	1.1	0.6	27.6	6.8	--	--
	08SM-63	--	NW	NW	9	41	6	572410	4652600	Tmbrh	B	49.46	1.30	18.13	8.04	2.94	0.17	5.23	8.55	3.65	0.80	0.57	1.45	100.19	11.20	4.3	854	26.2	136	228	90	99	8.4	18.9	86	105	34	532	17	44	<0.5	0.8	25	--	--	
	08SM-61	--	NW	NW	9	41	6	572420	4652670	Tmbrh	B	50.11	1.28	17.42	3.77	6.44	0.18	5.58	7.89	3.86	0.92	0.54	1.12	99.31	10.93	9.2	762	26.3	128	235	93	130	6.7	18.4	112	99	37	562	16	36	<0.5	2.3	25	--	--	
	SR-135	--	NE	NE	29	40	6	571740	4657450	Tmbrh	B	50.38	1.38	17.69	3.00	6.98	0.17	5.42	8.40	3.71	1.03	0.57	0.74	99.47	10.76	8.6	704	27.3	130	239	70	102	10.1	21.2	72	80	28	553	19.8	47.5	0.2	1.6	24.4	8.6	--	--
	04SM-82	--	SE	SE	20	40	6	571920	4657590	Tmbrh	B	50.43	1.34	17.48	6.93	3.33	0.18	4.78	8.43	3.60	1.06	0.57	1.17	99.30	10.63	12.2	741	29.3	132	178	70	83	8	20.4	68	82	33	697	22	48	<0.5	1.6	24	5	--	--
	08SM-64	--	NW	NW	9	41	6	572410	4652600	Tmbrh	B	50.44	1.37	17.43	6.07	4.60	0.17	5.54	8.34	3.61	1.21	0.58	1.19	100.55	11.18	10.4	1026	2																		

Table 1 (page 2).

Map no.	Sample no.	K-Ar Age(°)	1/4 Sec of 1/4	R. T. (S.)	UTM E (E.)	UTM N	Unit	Lith.	SiO ₂	TiO ₂	Al ₂ O ₃	Fe ₂ O ₃	FeO	MnO	MgO	CaO	Na ₂ O	K ₂ O	P ₂ O ₅	LOI (%)	Total (%)	FeO:Ti	Rb	Sr	Y	Zr	V	Ni	Cr	Nb	Ga	Cu	Zn	Co	Ba	La	Ce	U	Th	Sc	Pb	Yb	Be		
45	CN04-37	--	SW	SE	7	40	6	569730	466900	Tmbam	BA	53.23	1.13	17.68	2.68	6.01	0.16	4.12	7.57	3.86	1.26	0.66	1.12	99.48	9.36	14.4	670	63.2	178	151	42	57	13.2	19.8	71	87	27	723	--	--	<0.5	1	22	8	--
46	CN04-36	--	NW	NW	17	40	6	569250	466070	Tmbam	BA	53.26	1.14	17.21	3.46	5.62	0.17	4.39	7.57	3.62	1.48	0.69	1.01	99.62	9.71	12.1	721	32.1	172	124	38	45	11.1	21.1	69	76	24	798	--	--	0.6	1.3	18	8	--
47	CN04-36	--	SW	NW	17	40	6	570510	466020	Tmbam	BA	53.31	1.13	17.50	3.05	5.64	0.16	4.59	7.71	3.79	1.44	0.65	0.79	99.76	9.32	12.3	644	28.6	177	158	37	98	13.6	20.2	77	82	23	624	23	48	0.6	2.5	20	7	--
48	CN04-36	--	SE	SE	12	40	6	568420	466090	Tmbam	BA	53.31	1.12	17.87	2.68	6.23	0.17	4.63	7.58	3.68	1.53	0.70	1.00	100.20	9.60	13.9	663	38.4	182	171	41	71	13.4	20.2	69	81	21.5	623	27	81	2.13	21.3	10.4	--	--
48	CN04-36	--	SE	SE	12	40	6	571370	466120	Tmbam	BA	53.31	1.12	17.88	3.63	4.60	0.17	4.65	7.47	3.88	1.54	0.67	1.15	99.88	9.94	12.7	661	38.4	182	171	41	71	13.4	20.2	69	81	21.5	624	32	51	2.1	2.9	20	8	--
49	CN04-36	--	NW	SE	17	40	6	571550	465960	Tmbam	BA	54.10	1.11	17.34	1.64	6.70	0.16	4.53	7.46	3.55	1.56	0.67	0.86	99.68	9.09	15.7	648	26.9	184	159	40	52	11.8	20.1	83	84	25	713	18	48	0.9	0.9	19	7	--
50	CN04-36	--	NE	NW	8	40	6	570940	466220	Tmbam	BA	54.41	1.11	17.78	2.55	5.66	0.16	3.72	7.27	3.63	1.54	0.63	1.14	99.60	8.84	15.6	667	97.2	180	158	22	31	14.2	20.1	81	84	21	689	--	--	0.5	0.9	19	8	--
51	CN04-41	3.79 ± 0.10	NE	NW	1	40	5	567350	466300	Tpbac	B	50.74	1.11	16.46	2.05	6.15	0.14	6.91	9.94	3.12	1.47	0.83	99.43	9.84	15.6	667	97.2	180	158	22	31	14.2	20.1	81	84	21	689	--	--	0.5	0.9	19	8	--	
52	S97-87	3.85 ± 0.10 ^a	NW	NW	12	40	5	567210	466150	Tpbac	B	51.92	1.04	17.84	4.35	4.10	0.16	5.89	8.29	3.80	0.86	0.39	0.94	100.26	9.61	9.8	690	50.4	105	193	87	63	7.2	9.6	72	81	27	548	42.6	34	1.4	1.1	21.3	94	--
53	S97-73	3.44 ± 0.12	SW	NW	2	40	5	566620	466240	Tpbac	B	55.90	1.05	17.70	3.55	4.12	0.13	6.80	7.66	4.09	1.05	0.29	0.83	100.17	9.61	13.7	770	28.3	106	177	26	73	7.4	21.9	34	17	45.4	18.2	34.7	1.5	2.3	22	6.4	--	
54	S97-77	--	NW	SE	6	40	5	569800	466300	Tpbac	B	50.13	0.99	17.22	2.37	7.07	0.16	8.59	8.52	3.10	0.41	0.16	1.44	100.12	10.19	4.6	501	22.8	71	175	156	453	38	16.9	65	72	37	222	6	15	1	26	4	--	
55	S97-43	--	NW	SE	5	40	6	570830	466310	Tpbac	B	50.17	0.99	17.25	4.27	5.51	0.16	8.18	9.12	3.14	0.41	0.16	1.44	99.99	10.39	3.8	476	17.2	59	206	147	3.6	17.4	68	73	37.3	41	16.2	1.3	1.5	26.6	7.4	--		
56	S97-43	--	SE	SE	5	40	6	571910	466260	Tpbac	B	50.64	1.10	17.78	3.32	5.23	0.16	5.98	9.89	3.25	0.94	0.30	1.03	99.71	9.13	6.2	925	39.1	116	203	51	145	7.2	20.1	79	76	26	785	29	41	0.8	2.3	25	6	--
57	S97-102	--	SW	NE	11	40	5	566220	4661740	Tpbac	B	50.72	1.09	16.23	3.53	4.80	0.15	6.91	9.58	3.13	1.52	0.54	1.22	99.42	8.86	25.4	1293	31.9	172	87	241	71	196	36	73	28	419	13	30	1.1	2.9	23	5	--	
58	S97-92	--	NW	NE	11	40	5	569170	466350	Tpbac	B	50.80	1.11	17.71	5.77	4.14	0.16	6.88	8.30	3.17	0.49	0.17	1.52	100.22	10.37	15.5	664	31	88	156	51	60	4.1	20.4	50	71	24	596	--	--	1.8	0.9	18	5	--
59	CN04-32	--	NW	SE	5	40	6	571460	466310	Tpbac	BA	51.94	0.96	17.95	1.95	6.62	0.15	6.60	8.42	3.23	0.57	0.22	0.99	99.60	9.31	7.9	657	18.4	63	197	104	198	3	19.6	87	77	34	397	--	--	<0.5	<0.5	24	5	--
60	S97-95	--	NW	SW	5	40	6	570640	466280	Tpbac	B	50.93	1.08	17.66	2.02	6.22	0.15	5.97	10.09	3.27	0.99	0.39	0.93	99.70	8.93	9.3	928	23.5	114	210	49	150	7.6	19.2	95	74	24	737	22	46	1.7	2.8	27	5	--
61	S97-99	--	NW	SW	9	40	6	572090	4661810	Tpbac	B	51.32	1.08	17.51	2.97	5.36	0.15	5.86	9.78	3.33	1.10	0.39	0.71	99.56	8.93	13.5	909	24.1	115	176	50	145	7.6	19.3	81	70	25	630	16	45	1.7	3	24	6	--
62	CN04-31	--	SW	NW	6	40	6	569020	466230	Tpbac	B	51.55	1.22	17.64	4.80	4.88	0.16	5.98	8.30	3.35	0.61	0.30	0.69	99.48	10.22	13.9	682	18.3	85	180	55	74	4	20.2	37	71	25	428	--	--	<0.5	1.4	21	5	--
63	S97-88	--	SE	SE	5	40	5	567760	466240	Tpbac	B	51.72	0.96	17.18	4.00	4.47	0.15	6.33	9.14	3.56	0.80	0.35	0.49	99.75	8.97	8.7	824	20.6	97	172	87	241	71	196	36	73	28	419	13	30	1.1	2.9	23	5	--
64	CN04-49	--	SE	SE	5	40	5	567160	466450	Tpbac	B	51.87	1.00	17.50	2.67	4.47	0.16	6.85	7.77	3.20	0.63	0.21	1.31	99.64	8.86	8.8	626	31	88	156	51	60	4.1	20.4	50	71	24	596	--	--	1.2	<0.5	23	5	--
65	CN04-27	--	NW	SE	5	40	5	567140	466310	Tpbac	BA	51.94	0.96	17.95	1.95	6.62	0.15	6.60	8.42	3.23	0.57	0.22	0.99	99.60	9.31	7.9	657	18.4	63	197	104	198	3	19.6	87	77	34	397	--	--	<0.5	<0.5	24	5	--
66	S97-70	--	NW	NW	12	40	5	566870	466280	Tpbac	BA	52.04	0.95	17.99	4.32	4.77	0.16	5.87	8.29	3.81	0.84	0.39	1.06	100.59	9.62	7.6	687	32.4	105	205	83	143	9	19.6	86	82	27	477	28.9	46.4	0.5	0.9	24.1	8.3	--
67	S97-72	--	NE	NW	12	40	5	567390	466290	Tpbac	BA	52.10	1.04	17.91	3.88	5.09	0.15	6.03	8.53	3.87	0.86	0.39	0.48	100.33	9.54	8.5	677	21	113	188	83	151	19.8	61	71	31	455	16.4	39.5	0.7	1.1	24.7	6.1	--	
68	S97-87	--	NE	SW	1	40	5	567730	4662870	Tpbac	BA	52.86	0.89	17.51	3.70	5.12	0.16	6.25	7.76	3.64	0.72	0.22	0.57	99.40	9.39	9.1	687	44.8	77	155	80	158	4	19.7	33	72	29	411	12	24	1	1.4	20	4	--
69	CN04-11	--	NE	NE	11	40	5	566880	466200	Tpbac	BA	53.13	0.88	18.32	2.18	6.07	0.14	6.09	8.08	3.86	0.77	0.22	0.76	100.48	9.93	8.9	696	15	65	179	78	124	4	19.3	46	67	37	404	11	29	0.5	3.2	--	--	
70	S97-88	--	SE	NE	2	40	5	565910	466320	Tpbac	BA	53.20	0.83	18.09	1.88	6.29	0.15	5.59	7.55	3.69	0.72	0.22	1.41	99.72	8.87	8.7	677	30.8	81	157	74	148	19.2	39	71	28	435	18	29	<0.5	0.9	21	4	--	
71	CN04-12	--	NE	NE	11	40	5	566870	466280	Tpbac	BA	53.23	0.89	18.03	2.55	5.81	0.14	5.84	8.00	3.71	0.76	0.22	0.53	99.71	9.01	11	690	15	65	179	80	126	41	19.7	36	70	372	10	33	0.8	1.3	--	--		
72	S97-93	--	SE	NW	1	40	5	567390	466290	Tpbac	BA	53.42	0.95	18.20	1.98	6.34	0.14	5.39	7.89	3.84	0.74	0.22	0.93	99.73	7.95	12.3	779	20.4	106	165	23	83	7.1	19.4	73	18	469	13	38	1.4	2.6	20	6	--	
73	S97-74	--	NE	SW	12	40	5	567670	4661530	Tpbac	BA	54.01	0.93	18.39	3.12	4.93	0.13	5.17	7.83	4.03	0.85	0.22	0.63	100.22	8.60	11.4	675	20.6	82	158	68	94	5.6	19.7	64	74	28	407	11.6	20.4	0.9	1	23.4	5.6	--
74	S97-58	--	NE	NW	13	40	5	567440	4660770	Tpbac	BA	54.13	0.93	18.51	3.74	4.30	0.13	4.85	7.84	4.07	0.86	0.22	0.85	100.43	8.52	12.1	692	13.8	74	178	60	91	4.7	19.9	47	79	22	388	9.3	32.2	0.6	2.9	21.3	8.8	--
75	CN04-33	--	SE	SE	11	40	5	566790	4661130	Tpbac	BA	54.44	0.96	18.52	2.47	5.36	0.14	4.50	7.72	4.06	0.91	0.22	0.78	100.08	8.43	11.5	696	23	80	188	47	77	4	19.8	64	70	2	467	15	35	0.5	2.7	--	--	
7																																													

Table 1 (page 3).

Map no.	Sample no.	K-Ar Age ¹ (Ma)	1/4 of 1/4	Sec T	R	UTME (E)	Unit	Lith.	SiO ₂	TiO ₂	Al ₂ O ₃	Fe ₂ O ₃	FeO	MnO	MgO	CaO	Na ₂ O	K ₂ O	P ₂ O ₅	Total FeO ²	LOI (%)	FeO ³	Rb	Sr	Y	Zr	V	Ni	Cr	Nb	Ga	Cu	Zn	Co	Ba	La	Ce	U	Th	Sc	Pb	Yb	Ba									
106	S97-53	--	NE	SE	25	40	5	568250	465650	Tpbr	B	48.88	1.03	18.55	4.59	4.79	0.16	6.57	10.19	3.38	0.34	0.19	0.97	100.64	9.91	3.8	567	19.5	65	210	117	164	4.3	18.1	76	72	34	206	6.6	22.4	0.4	1.1	30.2	6.2	--	--						
107	CW04-30	--	NW	NW	5	40	6	570750	466370	Tpab	BA	53.79	0.94	17.83	1.85	6.13	0.14	4.52	7.98	3.77	0.87	0.23	1.29	99.64	8.66	8	573	35.5	93	142	70	102	4.6	19.8	73	74	34	406	--	--	<0.5	2.7	24	5	--	--						
108	S97-22	2.4 ± 0.2	SE	NE	3	40	5	566230	466370	Tpbc	B	50.40	1.11	18.30	3.33	6.11	0.17	7.45	9.35	3.51	0.43	0.25	1.03	100.44	10.12	0.9	577	23	82	210	109	222	3.9	17.1	75	69	41	264	13	33	0.9	<0.5	--	--	--	--						
109	CW11-3	--	NW	NW	11	40	5	563390	466240	Tpbc	B	48.76	1.09	17.57	2.07	7.34	0.17	8.08	10.11	2.95	0.31	0.20	0.75	99.18	10.23	3.8	450	18.5	68	195	114	248	4.4	16.9	83	67	34	196	5	22	0.2	0.2	--	--	--	--						
110	04SM-42	--	NW	SW	10	40	5	563840	466090	Tpbc	B	49.17	1.19	17.77	2.87	7.15	0.17	7.45	9.15	3.14	0.25	1.25	99.97	10.82	4.4	520	30.5	84	173	113	141	4.4	17.9	70	68	41	295	--	--	<0.5	1.1	25	--	--	--							
111	04SM-43	--	SE	NE	16	40	5	563570	466020	Tpbc	B	49.18	1.27	17.61	2.94	7.20	0.18	7.78	9.06	3.14	0.38	0.28	0.91	99.93	10.94	5.6	501	24.9	91	186	135	184	3.9	18.1	300	68	45	218	--	--	0.7	<0.5	29	4	--	--						
112	S97-50	--	SE	SW	3	40	5	564350	466250	Tpbc	B	50.03	1.19	17.74	3.01	6.62	0.17	7.21	9.02	3.44	0.42	0.26	0.83	100.14	10.59	4.2	490	26.6	88	209	99	190	5	17.7	74	73	34.4	196	10.2	20.1	1.3	1.7	28.6	5.9	--	--						
113	S95-30	2.57 ± 0.24	NW	NW	23	40	5	566650	465740	Tpbc	BA	52.32	0.79	17.59	2.73	5.17	0.14	6.01	10.63	3.41	0.47	0.14	0.64	100.33	8.48	6.8	678	14.1	47	224	48	155	4	18.5	35	66	27	195	18.5	25.5	0.9	1.3	28.9	5.1	--	--						
114	S97-42	--	NW	SW	25	40	5	567130	465670	Tpbc	B	49.01	1.30	17.29	5.23	6.34	0.17	6.10	9.51	3.68	0.41	0.30	1.24	100.58	11.16	1.7	476	36.3	96	212	121	137	6.2	17.9	76	74	39	264	14.5	26.7	<5	1.5	26.2	5.1	--	--						
115	CW8-10	--	NE	SE	15	40	5	565330	466010	Tpbc	B	49.11	1.20	17.78	2.39	7.46	0.17	7.53	9.15	3.24	0.42	0.25	0.58	99.28	10.68	4.4	513	21	79	216	113	157	4.6	18.3	43	68	33	200	8	22	0.8	0.5	--	--	--	--						
116	CW7-10	--	NW	SE	14	40	5	566210	465970	Tpbc	B	49.24	1.17	17.89	4.02	6.03	0.16	7.24	9.30	3.29	0.41	0.24	0.72	99.71	10.72	4.2	511	34	77	218	118	184	5.9	17	67	70	38	259	20	26	0.5	0.4	--	--	--	--						
117	CW8-3	--	SW	SW	14	40	5	565440	465930	Tpbc	B	49.38	1.20	18.06	5.24	6.91	0.16	7.05	9.33	3.50	0.44	0.24	0.76	100.27	10.70	1.8	530	25	80	238	115	186	4.1	17.4	71	68	40	227	13	31	0.5	2.3	--	--	--	--						
118	CW8-11	--	NW	NW	14	40	5	565420	466040	Tpbc	B	50.36	0.86	16.56	2.89	5.34	0.15	10.07	9.51	2.91	0.56	0.22	0.69	100.12	8.82	5	662	19	68	216	180	472	4.7	16.8	70	67	38	285	15	38	0.7	2.3	--	--	--	--						
119	CW2-5	--	NE	SE	6	40	5	566960	465650	Tpbc	B	50.45	0.82	18.62	3.65	5.01	0.15	6.94	10.70	2.86	0.24	0.13	1.71	100.76	9.22	--	628	19	55	231	49	161	4.1	18.3	66	68	37	240	14	28	0.5	3.2	--	--	--	--						
120	S97-3	--	SE	SE	16	40	5	565310	465910	Tpbc	B	50.46	0.77	17.90	2.09	6.28	0.15	6.93	10.70	2.70	0.31	0.15	0.93	99.37	9.07	2.7	580	15.7	50	232	52	178	3.7	18.3	76	67	29.6	210	7.7	22.9	1.3	1.1	28.8	7	--	--	--	--				
121	CW8-5	--	NE	SW	14	40	5	565930	466020	Tpbc	B	50.89	1.10	19.23	9.19	6.84	0.15	4.72	8.46	3.51	0.67	0.30	1.85	100.91	10.12	0.9	711	20	60	185	125	219	5.3	19.8	71	79	44	468	12	31	0.5	2.4	--	--	--	--						
122	S95-32	--	NW	SE	24	40	5	567920	465920	Tpbc	B	51.23	0.79	18.05	6.74	1.82	0.15	6.70	10.62	2.86	0.46	0.14	0.56	100.12	8.76	7	641	16.3	71	265	65	204	3.7	17.8	75	71	31	178	8.6	18	0.3	1.3	32.7	4.4	--	--	--	--				
123	CW2-2	--	SW	NW	24	40	5	567020	465930	Tpbc	B	51.40	0.78	18.10	2.13	6.04	0.15	6.81	10.46	2.86	0.43	0.14	1.09	100.39	8.84	2.4	603	17	53	224	43	146	3.8	18.6	72	61	34	247	10	25	0.5	2	--	--	--	--	--	--				
124	CW8-9	--	NW	NW	14	40	5	565710	466040	Tpbc	B	51.51	1.02	17.57	5.34	3.54	0.15	6.08	8.63	3.42	0.81	0.31	1.30	99.68	9.27	7.9	715	16	67	209	105	166	5.2	17.9	76	78	29	375	10	36	0.5	0.9	--	--	--	--	--	--				
125	S97-26	--	NW	NW	36	40	5	567230	465970	Tpbc	B	51.55	0.78	18.24	3.44	4.93	0.15	6.77	10.34	2.98	0.42	0.14	1.04	100.78	9.92	2.7	589	17	60	222	51	168	3.6	17.5	55	67	32	180	8	22.6	0.7	1.7	31.9	4.3	--	--	--	--	--	--		
126	04SM-52	--	NE	NE	21	40	5	563250	465930	Tpbc	B	51.60	0.79	17.95	2.11	6.15	0.15	6.34	10.37	2.70	0.41	0.16	1.16	99.89	9.94	6.2	603	17.5	62	205	43	130	2.9	18.4	65	64	33	200	--	--	<0.5	<0.5	29	4	--	--	--	--				
127	CW9-2	--	SW	SW	11	40	5	565100	466100	Tpbc	B	51.62	1.01	17.61	3.53	5.14	0.15	6.55	8.91	3.24	0.84	0.29	0.81	99.70	9.24	7.7	713	18.1	74	221	98	206	5	18.6	87	76.4	33	314	9.5	28.8	1.2	1.5	25.2	5.4	--	--	--	--	--	--		
128	CW4-8	--	SE	SW	23	40	5	565650	465760	Tpbc	B	51.66	0.78	18.04	2.20	5.89	0.15	6.65	10.50	2.87	0.48	0.14	0.88	100.24	8.75	4.5	599	17	54	228	43	147	3.5	18.5	91	62	34	212	12	37	0.9	1.8	--	--	--	--	--	--	--	--		
129	CW8-6	--	SE	NW	14	40	5	565660	4660130	Tpbc	B	51.76	1.02	18.13	5.84	3.06	0.14	6.09	8.65	3.67	0.80	0.29	0.88	100.33	9.24	5.3	792	16	63	253	90	146	4.9	18.9	64	71	33	394	15	38	0.5	1.9	--	--	--	--	--	--	--	--		
130	CW4-5	--	NW	SE	23	40	5	566200	4659180	Tpbc	B	51.87	0.77	17.80	2.87	5.13	0.14	7.14	10.45	2.93	0.48	0.13	0.62	100.33	8.57	4.3	641	18	50	227	60	167	3.6	17.6	56	61	32	218	9	22	0.5	2.2	--	--	--	--	--	--	--	--		
131	CW7-8	--	NE	NW	23	40	5	565780	4659040	Tpbc	BA	52.02	0.76	17.94	2.51	6.22	0.15	6.82	10.62	2.97	0.47	0.14	0.52	100.88	8.27	6.2	604	18.4	60	202	47	154	3.4	17.6	81	68	30	206	10	34	0.9	2.9	--	--	--	--	--	--	--	--		
132	S97-45	--	NE	SW	25	40	5	567730	4656820	Tpbc	BA	52.05	0.74	17.74	2.69	5.02	0.14	6.98	10.45	3.03	0.50	0.13	0.61	100.08	8.27	6.2	641	18.4	60	202	47	154	3.4	17.6	81	68	30	206	10	34	0.9	2.9	--	--	--	--	--	--	--	--		
133	CW8-7A	--	NW	NW	14	40	5	565660	4660660	Tpbc	BA	52.09	1.04	18.18	7.78	1.66	0.15	6.35	8.47	2.71	0.78	0.30	1.03	100.54	9.62	5.7	725	20	67	207	127	203	5.2	18.2	35	81	34	372	13	30	0.5	2.4	--	--	--	--	--	--	--	--		
134	CW9-5	--	NE	SW	11	40	5	565460	466130	Tpbc	BA	52.14	1.04	17.74	4.11	4.61	0.14	6.79	8.15	3.70	0.84	0.32	0.79	100.37	9.23	6.3	774	17	71	206	109	179	5.1	18.8	107	74	32	401	11	35	1.1	1.9	--	--	--	--	--	--	--	--		
135	CW6-2	--	NE	SW	26	40	5	566050	4660500	Tpbc	BA	52.18	0.78	17.81	1.98	5.90	0.15	7.00	8.50	2.93	0.52	0.14	0.85	100.80	9.54	5.1	636	16	53	221	49	163	3.7	17.3	91	64	34	193	6	18	0.5	2.5	--	--	--	--	--	--	--	--	--	--
136	CW2-3	--	NW	NW	23	40	5	565880	4659700	Tpbc	BA	52.33	0.83	17.46	2.00	5.98	0.15	6.98	10.31	3.02	0.57	0.17	0.88	100.71	8.65	4.8	611	16.3	62	188	55	188</																				

Table 1 (page 4).

Map no.	Sample no.	K-Ar Age ^a (Ma)	1/4	1/4 Sec	T. (S.)	R. (E.)	UTM N	Unit	Lith.	SiO ₂	TiO ₂	Al ₂ O ₃	Fe ₂ O ₃	FeO	MnO	MgO	CaO	Na ₂ O	K ₂ O	P ₂ O ₅	LOI (%)	Total Fe ₂ O ₃	Rb	Sr	Y	Zr	V	Ni	Cr	Nb	Ga	Cu	Zn	Co	Ba	La	Ce	U	Th	Sc	Pb	Yb	Be			
167	04SM-48	--	SW	NE	34	40	5	564900	465240	Tpdp	B	49.41	0.63	18.28	4.56	3.73	0.15	7.05	11.98	2.46	0.22	0.10	0.87	99.44	8.71	3.6	449	16.5	46	186	82	220	2.2	16.2	65	55	38	123	--	--	<0.5	<0.5	31	4	--	--
168	04SM-46	--	SE	NE	33	40	5	563440	465350	Tpdp	B	49.44	0.79	18.42	7.81	1.61	0.17	6.96	11.21	2.53	0.26	0.11	0.47	99.78	9.60	3.6	439	18.6	54	196	80	197	2.3	16.8	75	58	40	124	--	--	<0.5	<0.5	34	3	--	--
169	04SM-51	--	NE	NW	33	40	5	562560	465520	Tpdp	B	49.47	0.66	18.86	4.12	4.41	0.15	7.25	11.17	2.38	0.24	0.11	1.55	100.37	9.02	3.7	442	20.7	47	174	92	197	2.2	16.9	71	68	38	188	--	--	0.9	1.3	28	3	--	--
170	CW6-6	--	SE	SE	35	40	5	566980	4654500	Tpdp	B	49.55	0.77	18.07	3.41	5.46	0.16	7.63	11.6	2.71	0.26	0.11	0.98	100.66	9.48	--	446	18	51	247	80	210	3.2	17	87	58	33	238	10	16	0.5	1.9	--	--		
171	CW5-2	--	NW	NW	35	40	5	565610	4655820	Tpdp	B	49.81	0.75	18.14	2.03	6.47	0.16	8.01	11.55	2.74	0.28	0.11	0.58	100.63	9.22	0.5	442	19	49	242	70	202	2.6	16.8	93	55	36	148	10	23	0.5	1.9	--	--		
172	96-2	3.23 ± 0.25	NE	NW	8	41	6	571180	4652600	Qls	B	49.9	1.02	18.16	2.28	6.92	0.15	7.17	9.77	3.32	0.42	0.15	0.56	99.82	9.97	4.9	548	20	63	227	113	133	2.9	21.7	91	66	38	254	9	28	1.3	3.2	24	2.5	--	--
173	96-1	5.97 ± 0.23	NW	NE	8	41	6	571560	4652550	Qls	B	51.39	1.32	17.34	3.12	6.66	0.17	5.55	7.99	3.81	1.18	0.59	0.86	99.98	10.52	12.3	752	27	141	205	64	110	9.3	23.1	94	81	33	582	23	51	1.8	3.7	22	7.3	--	--
174	96-4	--	NW	SW	7	41	6	568980	4651830	Qls	BT/A	52.02	1.27	17.53	2.90	6.44	0.16	4.78	7.67	3.90	1.37	0.70	0.79	99.53	10.06	11.6	771	28	155	167	49	85	10.1	20.5	84	86	25	687	26	57	1.4	1.8	--	--		
175	JN97/67A ^a	--	NW	SW	14	48	3	567260	4650090	Qls	A	57.95	1.33	15.33	2.30	4.96	0.15	2.50	6.12	3.78	1.57	0.39	3.51	99.89	7.81	61.1	451	30.2	228	205	3.8	--	10.6	19.3	72	90	15.2	603	24.1	56.5	1.7	5.5	22	10.6	--	--